Dynamic Cracking and Energy Absorption in Laminates Containing Through-Thickness Reinforcement

Final Report for 08/30/99 -- 02/28/01
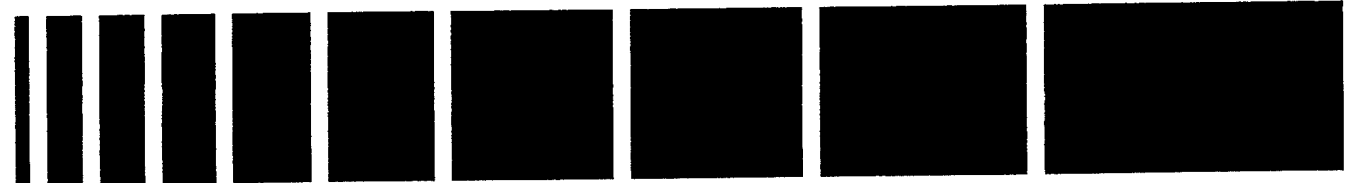
Contract No. DAAD19-99-C-0042

Prepared for:

U.S. Army Research Office
Attn: AMSRL-RO-RI
P.O. Box 12211
Research Triangle Park, NC 27709-2211

Prepared by:

B. Cox and S. Narayanaswamy
Rockwell Science Center
1049 Camino Dos Rios
Thousand Oaks, CA 91360

March 2001

20010517 048

**Rockwell
Science Center**

Copy # 3

REPORT DOCUMENTATION PAGE

Form Approved
OMB No. 0704-0188

1. AGENCY USE ONLY (Leave blank)	2. REPORT DATE 4/18/01	3. REPORT TYPE AND DATES COVERED Final Progress Report 8/30/99-2/28/01

4. TITLE AND SUBTITLE
Dynamic Cracking and Energy Absorption in Laminates Containing Through-Thickness Reinforcement

5. FUNDING NUMBERS
DAAD 19-99-C-0042

6. AUTHOR(S)
B.N. Cox and S. Narayanaswamy

7. PERFORMING ORGANIZATION NAME(S) AND ADDRESS(ES)
Rockwell Science Center
1049 Camino Dos Rios
Thousand Oaks, CA 91360

REGISTERED APR 3 0 2001

8. PERFORMING ORGANIZATION REPORT NUMBER

9. SPONSORING/MONITORING AGENCY NAME(S) AND ADDRESS(ES)
U.S. Army Research Office
PO Box 12211
REsearch Triangle Park, NC
27709-2211

10. SPONSORING/MONITORING AGENCY REPORT NUMBER
40342.1-MS

11. SUPPLEMENTARY NOTES
The views, opinions and/or findings contained in this report are those of the author(s and should not be construed as an official Dept. of the Army position, policy or decision, unless so disignated by other documentation.

12a. DISTRIBUTION/AVAILABILITY STATEMENT
Approved for release; distribution unlimited.

12b. DISTRIBUTION CODE

13. ABSTRACT (Maximum 200 words)
We report several fundabmental results in the delamination resistance of through-thickness reinforced structures under dynamic load conditions. The main results are: (1) An elaborate micromechanical model shows how a bridging tow should behave if it is initially inclined to the fracture plane and subject to mixed mode quasistatic loading (2)A bridging law for fiber reinforced composites under dynamic crack propagation conditions has been derived. INertial effects in the mechanism of fiber pullout during dynamic propragation of a bridged crack are critically examined for the first time. (3) The dynamic delamination cracking behavior and the energetics of crack growth in through thickness double cantilever beam specimens has been analyzed. Steady state crack growth is attainable provided certain conditions are satisfied. Guidelines for design of experiemtns to probe the efficacy of bridging on improving the dynamic fracture toughness of through tickness reinforced structures are established. In summary, these results form a sound fundamental basis for design and life prediction of through thickness reinforced structures.

14. SUBJECT TERMS

15. NUMBER OF PAGES
98

16. PRICE CODE

17. SECURITY CLASSIFICATION OF REPORT	18. SECURITY CLASSIFICATION OF THIS PAGE	19. SECURITY CLASSIFICATION OF ABSTRACT	20. LIMITATION OF ABSTRACT
UNCLASSIFIED	UNCLASSIFIED	UNCLASSIFIED	UL

Table of Contents

Section **Page**

List of Figures

1. INTRODUCTION

This final report covers the period August 30, 1999 through February 28, 2001. We summarize our progress in determining the delamination resistance of through thickness reinforced structures under dynamic load conditions. Leveraging collaborations at Los Alamos National Lab and the University of Genova, Italy and a subcontract with Dr. Ares Rosakis (ETECH Inc.) for dynamic push-in experiments will also be described.

Our progress in this reporting period has resulted in eight papers written or in preparation [1-8]. We are especially pleased with some fundamental results that we have derived with simple analytical models. The models have yielded particularly insightful results for general combinations of properties of the matrix and the through thickness reinforcement, crack velocity, loading configurations, elastic anisotropy, and bridging parameters.

Highlights of our accomplishments are as follows.

(i) Through-thickness reinforcement is a promising solution to the problem of delamination susceptibility in laminated composites, but its acceptance by the design community awaits dependable models of its performance and failure to treat mixed mode loading cases and bridging tows that are canted relative to the delamination fracture plane. We have constructed elaborate micromechanical models that show how a bridging tow should behave if it is initially inclined to the fracture plane and subject to mixed mode quasistatic loading [1]. From these models, the effective bridging law for a bridged delamination crack can be derived. Approximations guided by experiments enable the results to be obtained in remarkably simple form, with closed form analytical expressions available for certain cases. The approach outlined above is an excellent starting point for studying dynamic delamination under mixed mode loading conditions.

(ii) The generalized model developed above should be applicable to all problems of monotonic loading and for general stress state. The model reveals that, provided pullout of the entire tow does not occur, shear bridging tractions are sustained more effectively by fibrous tows canted so that they will be loaded with the nap (tension along their axes)

1

than by tows canted so that they will be loaded against the nap. Pullout can be avoided either by using continuous stitching or, if short rods are used, by ensuring that the aspect ratio of the rod (length/circumference) is sufficiently large. Orienting fibrous tows to be loaded in axial tension exploits the high axial stiffness of the fibres in the tow. Orienting them so that they are initially in compression will cause initial fibre rotation by a mechanism analogous to kinking that depends primarily on the matrix strength and also maximises the tendency of the tow to deflect laterally through the laminate. Both of these mechanisms tend to create a softer response under shear bridging tractions.

(iii)   A bridging law for fiber reinforced composites under dynamic crack propagation conditions has been derived [2,3]. Inertial effects in the mechanism of fibre pullout during dynamic propagation of a bridged crack were critically examined for the first time. By reposing simple shear lag models of pullout as problems of dynamic wave propagation, the effect of the frictional coupling between the fibres and the matrix is accounted for in a fairly straightforward way. Analytical solutions were found to the problem of coupled waves that propagate away from the fracture plane of the bridged crack as the bridging tractions increase with time. These solutions yield the time-dependent relationship between the crack opening displacement and the bridging traction.

(iv)   With the aid of the dynamic pullout law derived above, simple criteria were determined for significant inertial effects in representative crack propagation problems. We find that inertial effects in the bridging mechanism will often be significant for a matrix crack propagating dynamically in the steady state ACK limit in a brittle matrix continuous fibre composite or for delamination in laminates reinforced by through-thickness stitching or rods. We also find that significant inertial effects are favoured by low fibre volume fraction, low friction stress, low matrix bar wave speed, and low fibre modulus; and high fibre diameter and high matrix modulus. If the fibre modulus is high enough (relative to the matrix modulus), the criterion for inertial effects becomes independent of fibre modulus. The matrix density enters the criterion only through the matrix bar wave speed. The criterion is always independent of the fibre density. Inserting values for typical stitched laminates, one finds that *dynamic effects will in fact be significant for many*

2

delamination crack propagation cases. Using a dynamic traction law rather than a law for static loading is therefore essential in general.

(v)   For pullout or bridging stresses that linearly increase in time, the instantaneous crack displacement is less in the presence of inertial effects than it would be under static loading to the same bridging stress. However, solutions for pullout from a rigid matrix suggest that, if the bridging stress rises rapidly and is then held at a constant value, the crack displacement when all particle motion finally stops will be greater than it would have been under static loading to that stress level. Thus regimes of both hardening and softening of the bridging traction law due to inertial effects can be expected in bridged crack problems.

(vi)   We also formulated fast numerical solutions for general loading cases and hence have a scheme to compute the bridging law for fairly general conditions [4]. This will be required to solve large-scale bridging, dynamic crack problems to self-consistency (bridging tractions unknown *a priori*). The history dependent bridging law thus computed will form the basic ingredient in the computation of the structural response of the composite under dynamic loading conditions.

(vii)   The dynamic delamination cracking behavior and the energetics of crack growth in through thickness double cantilever beam (DCB) specimens has been analyzed [5]. The double cantilever beam (DCB) specimen loaded dynamically by a flying wedge offers a relatively simple experimental approach to analyzing the mode I dynamic delamination problem. The role of bridging by stitches or rods on dynamic crack growth was computed by solving the bridged crack problem within the framework of beam theory. Analytical results were obtained for steady state crack propagation conditions.

(viii) The magnitude of the bridging traction, which is controlled by the properties of the through thickness reinforcement, plays a significant role in the crack growth behavior. For steady state crack growth conditions, different regimes of the solution behavior have

3

been identified which would correspond to different crack propagation characteristics. Critical velocities that demarcate the various solution regimes have been identified.

(ix) Steady state crack growth is attainable for this loading configuration provided certain conditions are satisfied. Regions of stable crack growth have been identified in terms of the material properties of the through thickness reinforcement, the size of the DCB specimen and the velocity of the wedge. This provides guidelines for design of experiments to probe the efficacy of bridging on improving the dynamic fracture toughness of through thickness reinforced structures [6].

(x) The dynamic crack energy release rate as a function of the local crack tip velocity has been computed for a material possessing orthotropic symmetry under general mixed mode loading conditions. The dynamic energy release rate varies as $O[(v_r - v)^{-1}]$ as $v \to v_r$, and where v is the crack speed and v_r is the Rayleigh wave speed. We find that the variation in the dynamic crack energy relese rate for orthotropic materials can be rationalized in terms of the orthotropy parameters λ and ρ, just as in the static case. This computation of the dynamic energy release rate is necessary to calculate the energetics of crack growth for standard engineering specimens [7].

(xi) An approximate formula for the static weight function that describes the crack tip stress intensity factor due to a pair of point loads on the fracture surface of an orthotropic delamination specimen has been postulated and validated numerically [8]. This weight function enables accurate solution of mode I delamination problems in the presence of large scale bridging over all crack length regimes, since it avoids the errors of beam theory in describing the singular crack tip fields. However, comparison of results for large scale bridging problems with a Dugdale (uniform traction) bridging law shows that a beam theory model with appropriate crack tip corrections (available in the literature) may be acceptably accurate. The weight functions will be used to formulate integral equation solutions, which will be to ensure that accurate results are always available at

4

least as a reference in future work. Extension to mode II loading and dynamic weight functions is under way.

(xii) A subcontract was issued to Etech, Inc. for experiments to gain understanding of the mechanics of fibre push-in (analogous to pullout) under dynamic loading. The first experiments have already been completed (Owen and Rosakis) and the key strain field and velocity data successfully recorded. Further reports will follow after proper analysis of the data.

Considerable headway has been made in all of the tasks listed above, even though the program has been in effect for only a short time period (~ 16 months). The work in each case is mainly finished and we are well advanced in writing papers. Unfinished mansucripts will be completed in the next few months.

2.0   FUTURE WORK

The following issues remain as the natural continuation of our work.

1.   The dynamic traction law model must be generalised to mixed mode loading. We have a model for mixed mode loading in the static case [1]. We now know from this year's work that dynamic effects are likely to be important in most cases and we therefore should consider how to adapt our static model to deal with inertial effects during mode II deflections of a stitch in a laminate.

2.   The fracture or crack propagation problem must be solved for mixed mode loading. We know from the static case that mode ratio effects have a major influence on the qualitative character of crack propagation in the presence of large scale bridging. This fundamental question must therefore also be resolved for dynamic fracture.

3.   We are now in position to map out (a) a method of predicting the extent of delamination damage during composite impact and (b) the energy absorption capacity of delaminating composites. In both cases, the outcome will be very strongly affected by the presence of through-thickness reinforcement (large scale bridging zones).

4.   Experimental data must be obtained and analyzed for dynamic crack and pullout problems to validate our theoretical results. Although there has been considerable experimental characterization of fibre - matrix debonding under quasi-static loading conditions, comparatively little is known regarding the process at relatively high, dynamic loading rates. Prof. Ares Rosakis of Caltech, with a sub-contract under this program, is conducting a detailed experimental study of the dynamic fiber pull-out / push-in process and will provide data with which the validity of the pull-out model will be assessed. Through the use of a carefully designed 2D model material system and

high-speed diagnostics, a complete quantitative description of process can be obtained which makes direct comparison with the model possible.

5. Upon passing of the crack tip, a debond crack propagates along the length of the fibre away from the fracture plane. Propagation of the debond crack is governed by the fracture energy associated with the separation of the matrix and the fibre at the debond crack tip and the work done against friction in displacing the debonded fibre along its axis. In many composites, the debond energy is small and pullout is dominated by friction over a wide range of pullout displacements. However, to deal with cases where this assumption is not true, we intend to develop a theoretical framework that incorporates the debond energy in the pullout model. Although, simple extensions of shear lag models are available to deal with debond energy contribution for the quasistatic loading case, the corresponding formalism for the dynamic case appears much more complicated and is yet to be developed.

6. Weight function or other computational formulations must be used to validate and extend analytical and illustrative results based on beam theory.

7. Based on our increasing understanding of the dynamic delamination process with large scale bridging, models of energy absorption in a laminate structure and delamination resistance must be formulated. Such models are intended to enable systematic optimisation of energy absorption and delamination resistance by providing reasonably simple but physically correct design rules.

These are the issues identified in our original proposal. We are very much on track to address them in their turn.

3.0 SUMMARY OF PROGRESS

3.1 Mechanics of Crack Bridging by Fiber Tows under Mixed Mode Loading

Through-thickness reinforcement is a promising solution to the problem of delamination susceptibility in laminated composites, but its acceptance by the design community awaits dependable models of its performance and failure. Models have been slow in coming, mainly because the mechanisms involved in the failure of through-thickness reinforcing elements are at first sight very complicated.

However, from a micromechanical standpoint, key mechanisms of damage recently revealed by detailed experiments show encouraging universality among bridging tows of various kinds, including stitches and short fibrous rods (so-called "z-fibers"). The key phenomena are as follows: The bridging tow deforms plastically in axial shear at the smallest observable crack sliding (mode II) displacements. Plasticity is mediated at first by crazing and microcracking in the resin within the tow. Plasticity and damage (microcracking, splitting, and spalling) occur soon after in the adjacent laminate. Plasticity allows fiber rotation near the delamination crack plane, so that the axial stress in the fibers creates significant shear components on the fracture plane (creating shear bridging tractions). By this mechanism, the mode II bridging tractions can reach ~ 1 GPa across the section of the tow, which is an order of magnitude higher than the tow could support in axial shear prior to fiber rotation. At small crack opening or sliding displacements, the tow also detaches via circumscribing matrix cracks (not necessarily fiber/resin debond cracks) from the surrounding composite. The debonded tow slides through the laminate and the debonded zone extends fairly quickly to the outer surface of the laminate. Sliding displacement can accommodate the increase in path length that occurs when the locus of the bridging tow is altered by fiber rotation. Fiber rotation in the bridging tow also implies lateral motion of the tow into the surrounding laminate. This ploughing action may be modeled phenomenologically as the problem of a punch being driven into a plastic medium, since the

8

laminate deforms by matrix mediated plasticity. The driving force for the punch deflection may be regarded as the combination of the line tension sustained by the fibers in the bridging tow in concert with their curvature, which increases as the tow deflects.

In this work, all of the phenomena described above has been modeled with remarkable simplicity, and without betraying the observed physics of the bridging process [1]. A model of the response of the bridging tow has been formulated and solved analytically, giving useful insight into the governing material and geometrical factors. The formulation is generalised to allow the bridging tow to be canted relative to the fracture plane and to deal with mixed mode loading conditions. The essential material property that came out of solving the mechanics of the bridged crack problem is the traction law, $p(u)$, relating the vector of relative displacements of the crack surfaces, u, to the vector of tractions, p, supplied to the fracture surfaces by the bridging through-thickness reinforcement. Generalizations to any combination of mode I and II displacements and tractions was considered to make it relevant to problems of interest. The mixed mode traction law was derived in analytical form, requiring at most the solution of two transcendental equations in a single scalar variable. The results contain only a few material parameters, including a shear flow stress for the bridging tow, a friction stress for tow sliding, and a punch resistance stress, all of which can be independently estimated. Reasonable values for the parameters lead to laws that agree very well with experimental measurements. Thus a good description is readily available for the physics of crack bridging in the static delamination crack problem.

The generalized model developed above should be applicable to all problems of monotonic loading and for general stress state. The model reveals that, provided pullout of the entire tow does not occur, shear bridging tractions are sustained more effectively by fibrous tows canted such that the tows are loaded with the nap (tension along their axes). Pullout can be avoided either by using continuous stitching or, if short rods are used, by ensuring that the aspect ratio of the rod (length/circumference) is sufficiently large. Orienting fibrous tows to be loaded in axial tension exploits the high axial stiffness of the fibres in the tow. Orienting them so that they are initially in compression will cause initial fibre rotation by a mechanism analogous to kinking that

depends primarily on the matrix strength and also maximises the tendency of the tow to deflect laterally through the laminate. Both of these mechanisms tend to create a softer response under shear bridging tractions.

To conclude, we have constructed an elaborate micromechanical model that shows how a bridging tow should behave if it is initially inclined to the fracture plane and subject to mixed mode loading. From these models, the effective bridging law for a bridged crack model of the delamination can be derived. Once again, approximations guided by experiments enable the results to be obtained in remarkably simple form, with closed form analytical expressions available for certain cases. The approach outlined above is an excellent starting point for studying dynamic delamination under mixed mode loading conditions.

3.2   Inertial effects in the pullout mechanism of a bridged crack

In this part of our research [2,3], it is our aim to develop an equivalent bridging model for individual through-thickness reinforcement tows under dynamic loading. Dynamic loading rates can significantly affect the mechanisms described above, probably leading to a hardening of the traction law and more brittle behavior of the bridging tow. In order to get insights into how dynamic effects modify the mechanics of deformation, we begin by modifying the mechanics of pullout under quasistatic loading to include the inertial effects.

The mechanics of pullout and the resulting traction law have been much studied and are well understood for static loading. Simple analytical forms are available for $p(u)$ when the frictional coupling of the reinforcement to the matrix is uniform and slip extends over distances that are large compared to the reinforcement diameter (Marshall, Cox, and Evans, 1985; McCartney, 1987). In this limit, which is a common case in ceramic composites and textile polymeric composites, the shear lag model of load transfer between the reinforcement and the matrix is accurate. Simple extensions of models of this class are also available to deal with small but nonzero levels of the work required to debond the reinforcement from the matrix prior to slip

[11]. Given the relationship, $p(u)$, the characteristics of crack propagation can be computed by solving a bridged crack problem [19-22].

In this section, we extend existing models of the mechanics of pullout to high loading rates. An approach to evaluating a traction law that takes account of the inertia of the reinforcement and the matrix is formulated as a direct extension of the elementary static loading model [9,10]. The chosen base model for static loading has proven consistent with experiments in many material systems and has been the foundation of major advances in understanding damage in composites. The spirit of the present work is to seek equivalent insight into dynamic damage by incorporating the influence of inertia into the simplest credible model. Thus not all aspects of the micromechanics of pullout that could be important in some cases will be addressed. Instead, attention will be focused on identifying a characteristic time for the frictional pullout problem that will allow rapid assessment of when inertial effects will be important.

Idealization of the Bridged Crack problem

The crack propagation and pullout problems are depicted schematically in Fig. 1. A matrix crack propagates on the plane $z = 0$ and is bridged by intact fibres in its wake. (For simplicity of expression, the term fibre from here on will be used to refer to bridging entities of any kind, including stitches, rods, and bridging grains.) Upon the passing of the crack tip, a debond crack propagates along the length of each fibre away from the fracture plane. Propagation of the debond crack is governed by the fracture energy associated with the separation of the matrix and the fibre at the debond crack tip and the work done against friction in displacing the debonded fibre along its axis. In many composites, the debond energy is small and pullout is dominated by friction over much of the range of pullout displacements. Therefore, in this first model the debond energy will be ignored.

For static loading, the crack propagation problem can be idealised by replacing the process zone by elastic composite material down to the fracture plane and representing the phenomena within the process zone by bridging tractions applied continuously on the fracture surfaces (Fig. 1). The

bridging tractions, p, are related to the axial stress, T, in the fibres at the fracture plane by $p = fT$, where f is the area fraction of the fibres on the plane $z = 0$. For aligned continuous reinforcement, f is also the volume fraction of the fibres. The total crack opening displacement, $2u$, in the idealisation should be defined as the difference in the actual displacement evaluated across the process zone and the displacement that would be expected if the material in the process zone was elastic.

(a)

(b)
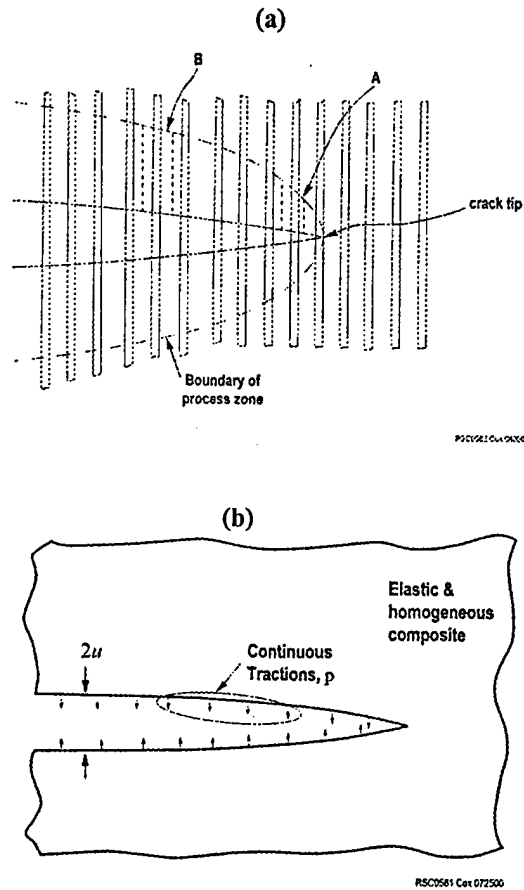
Figure 1. (a) Schematic of a crack bridged by fibres, showing process zone where relative displacement exists between fibres and matrix. (b) Idealization of the bridged crack problem with process zone replaced by surface tractions acting on the fracture surfaces.

The traction law, $p(u)$, is derived by considering the micromechanics of the phenomena occurring within the process zone, which is to say the micromechanics of frictional sliding. The micromechanical problem can be represented by a small volume of material, e.g., the material

bounded by one of the dotted rectangles in Fig. 1a. The traction boundary conditions for the representative volume are as follows. At $z = 0$, the matrix is traction-free, while the fibres sustain the axial traction T. At $z = l_s$, the strain in the fibres and the matrix must equal the average strain in the composite adjacent to the process zone ($z > l_s$). Shear tractions may arise along the vertical boundaries of the representative volume (parallel to z), but these are neglected.

In the problem of a crack propagating under static loading, the traction at $z = l_s$ for the representative volume associated with a fixed volume of material is assumed to rise from zero when the material is immediately behind the crack tip to increasing values as the material passes further back into the wake [9]. The tractions are not truly zero right at the crack tip, since the fibres are not stress-free, but assuming they are leads to reasonable results for the bridged crack problem as long as the fibres remain intact over sufficiently long distances into the crack wake. Then shielding of the crack tip is dominated by the bridging tractions acting in the further crack wake, where the boundary conditions are correct. In dynamic loading, the boundary conditions at the boundary of the process zone involve displacement and displacement rates as well as stress or strain conditions.

The Micromechanics of Dynamic Pullout

When friction is the only active force of resistance, the static pullout problem reduces to an idealization in which fibers are pulled out of a half-space to which they are not initially bonded. The dynamic problem is one of wave propagation along a fibre in the presence of frictional retardation and with no debond crack tip or crack tip field to be considered.

The archetypal problem is illustrated in the figure 2 below. A representative volume consists of cylindrical fibres of radius R and volume fraction f embedded in a matrix ($z \geq 0$). The fibre and the matrix have axial Young's moduli E_f and E_m and densities ρ_f and ρ_m respectively. The axial displacement, strain, and stress of the fibre and the matrix are denoted u_f and u_m, ε_f and ε_m, and σ_f and σ_m, respectively. The axial displacements will be assumed to be the only nonzero displacement components induced by loading and to be uniform across any section of the fibre or

the matrix. Thus the displacement, strain, and stress in the fibre and the matrix are functions of z and t only. They are consistent with assuming that the friction forces are constant (unaffected by fibre contraction or dilation due to axial stresses).
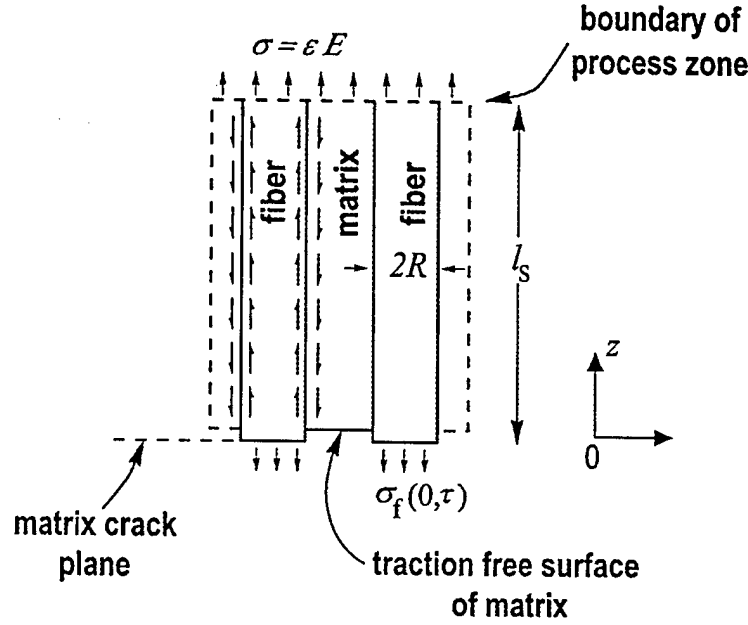
RSC0586 Cox 080500

Figure 2: Schematic of the dynamic pullout problem in a composite near the fracture plane.

There is no initial bond between the fibres and the matrix. The fibres are coupled to the matrix by friction tractions, τ_f, which are assigned the following properties. If relative motion exists between the fibres and the matrix, then

$$\tau_f = \tau \quad (\dot{u}_f < \dot{u}_m) \tag{3.2.1a}$$

$$\tau_f = -\tau \quad (\dot{u}_f > \dot{u}_m) \tag{3.2.1b}$$

where a dot indicates time differentiation, τ is a positive constant and $\tau_f > 0$ indicates friction tractions acting on the fibres in the positive z direction. When the fibres and the matrix are not in

14

relative motion, the friction tractions may support stress gradients in the fibres and the matrix, provided that the required magnitude of τ_f does not exceed τ. Thus, by equilibrium considerations,

$$\left|\frac{\partial \sigma_f}{\partial z} - \rho_f \frac{\partial \dot{u}_f}{\partial t}\right| \le \frac{2\tau}{R} \qquad \& \qquad \left|\frac{\partial \sigma_m}{\partial z} - \rho_m \frac{\partial \dot{u}_m}{\partial t}\right| \le \frac{2f}{1-f}\frac{\tau}{R} \qquad (\dot{u}_f = \dot{u}_m). \qquad (3.2.1c)$$

Here the possibility is included that the matrix and the fibres have the same non-zero velocity and may also be accelerating together, although such general solutions will not be exhibited in this paper. With such a friction law, the dynamic wave equations describing those parts of the fibres and the matrix that are in relative motion may be written approximately as

$$\frac{\partial^2 u_f}{\partial z^2} = -\frac{2\theta\tau}{RE_f} + \frac{1}{c_f^2}\frac{\partial^2 u_f}{\partial t^2} \qquad (3.2.2a)$$

and

$$\frac{\partial^2 u_m}{\partial z^2} = \frac{2f}{1-f}\frac{\theta\tau}{RE_m} + \frac{1}{c_m^2}\frac{\partial^2 u_m}{\partial t^2} \qquad (3.2.2b)$$

where $\theta = 1$ if $\dot{u}_m > \dot{u}_f$ and $\theta = -1$ otherwise; and c_f and c_m are the bar wave velocities in the fibres and the matrix, given by

$$c_f = \sqrt{\frac{E_f}{\rho_f}} \qquad \& \qquad c_m = \sqrt{\frac{E_m}{\rho_m}} \qquad (3.2.2c)$$

15

The approximation of using the bar wave velocities rather than the longitudinal wave velocities in the z direction in the wave equations is consistent with the simplified treatment of stresses and strains and the assumed uniformity of the friction stress.

Boundary conditions in the dynamic case are as follows. At the fracture plane,

$$u_f(0, t) = 0 \quad \& \quad \sigma_m(0, t) = 0 \quad (z = 0). \tag{3.2.3}$$

At the boundary of the process zone (limit of relative fibre/matrix motion),

$$u_f = u_m = u_c \quad (z = l_s) \tag{3.2.4}$$

where u_c is the displacement of the adjacent intact composite; and conditions also exist on stress or strain and particle velocities. These further conditions depend on the nature of the loading history, which can be expressed as the function $\varepsilon(t)$, where ε is the strain in the z direction in the intact composite adjacent to the process zone boundary. The bridging traction, p, is related to ε by

$$p = \varepsilon E \tag{3.2.5a}$$

where the composite modulus, E, is given by

$$E = fE_f + (1 - f)E_m \tag{3.2.5b}$$

In the depiction of Fig. 2, the process zone boundary will propagate away from the fracture plane as $\varepsilon(t)$ rises. In the case to be considered in this paper, $\varepsilon(t)$ will be assumed to rise continuously and monotonically from zero. Placing the origin of time, $t = 0$, at the onset of nonzero $\varepsilon(t)$, the location of the zone boundary at time t may then be written as:

$$l_s = \eta(t)c_m t \tag{3.2.6a}$$

16

where the function $\eta(t)$ depends on material and geometrical parameters and the form of $\varepsilon(t)$ and will be shown to be bounded by

$$0 < \eta(t) \leq 1 \qquad . \qquad (3.2.6b)$$

For the loading conditions considered, the additional boundary conditions at $z = l_s$ are:

$$\dot{u}_f = \dot{u}_m = \dot{u}_c \qquad (z = l_s) \qquad (3.2.7a)$$

and

$$\varepsilon_f = \varepsilon_m = \varepsilon(t) \qquad (z = l_s). \qquad (3.2.7b)$$

If the load history, $\varepsilon(t)$, possesses discontinuities, e.g., a step load, then discontinuities in stress and velocity will also propagate at the boundary of the process zone (e.g., Achenbach [12]).

Composite Stress Rising Linearly in Time

A case of representative interest for dynamic bridged crack problems and for which analytical results can be found is that of a load or bridging traction that increases linearly in time. A linearly increasing load might give insight, for example, into bridging effects in a specimen in which substantial bending arises, such as a standard double cantilever beam delamination specimen. In such specimens, the crack profile is often approximately linear and the rate of increase of the bridging tractions at any point might also be approximately linear if the crack propagates at approximately constant speed. The bridging traction at a particular material point might be expected to rise from zero as the delamination crack first passes until a peak value is reached, perhaps corresponding to bridging fibre rupture. Analytical results can be found for linearly increasing loads.

Let

$$\varepsilon(t) = kt \tag{3.2.8}$$

where k is constant and all displacements and boundary tractions are zero for $t < 0$. In this case, $\theta = 1$ and the wave equations have the solutions

$$u_f = -\frac{k}{c_m}\alpha z^2 + [1 + 2\eta\alpha]\varepsilon z \tag{3.2.9a}$$

$$u_m = \frac{k}{c_m}\frac{1}{2\eta}z^2 + \frac{1}{2}[1 + 2\eta\alpha]\varepsilon l_s \tag{3.2.9b}$$

where η is independent of time and satisfies

$$\alpha\eta^3 + \tfrac{1}{2}\eta^2 + \beta\alpha\eta - \tfrac{1}{2} = 0 \tag{3.2.9c}$$

with the dimensionless parameters α and β given by

$$\alpha = \frac{\tau c_m}{E_f R k} \qquad \& \qquad \beta = \frac{f}{1-f}\frac{E_f}{E_m} \tag{3.2.9d}$$

Analysis shows that Eq. (3.2.9c) has only one real root, which always lies in $(0,1)$.

The particle velocities and the strains for $0 \le z \le l_s$ are given by

$$\dot{u}_f = [1 + 2\eta\alpha]kz \tag{3.2.10a}$$

$$\dot{u}_m = [1 + 2\eta\alpha]kl_s \tag{3.2.10b}$$

$$\varepsilon_f = \left[1 + 2\eta\alpha\left(1 - \frac{z}{l_s}\right)\right]\varepsilon \tag{3.2.10c}$$

$$\varepsilon_{\mathrm{m}} = \frac{z}{l_{\mathrm{s}}} \varepsilon \qquad\qquad (3.2.10\mathrm{d})$$

The matrix particle velocity is uniform and increases in proportion to l_{s}. The fibre velocity rises linearly through the process zone. A strain concentration, $\varepsilon_{\mathrm{f}}/\varepsilon$, propagates in the fibre behind the process zone front, while the matrix strain in the process zone is always less than ε. The strain distributions and velocities beyond the process zone, $z > l_{\mathrm{s}}$, need not be specified, provided the composite strain ε obeys the condition Eq. (3.2.7) on the process zone boundary.

The displacement, u, to be used in defining the traction law, $p(u)$, is given by the common fibre and matrix displacement, $u_{1} = u_{\mathrm{f}}(z = l_{\mathrm{s}}) = u_{\mathrm{m}}(z = l_{\mathrm{s}})$ at the boundary of the process zone minus the displacement expected if the process zone material were elastic:

$$u = u_{1} - \varepsilon l_{\mathrm{s}}$$

$$= \frac{c_{\mathrm{m}}}{k} \alpha \eta^{2} \varepsilon^{2}$$

$$= \frac{c_{\mathrm{m}} \alpha \eta^{2}}{k E^{2}} p^{2} \qquad\qquad (3.2.11)$$

Equation (3.2.11) constitutes the traction law for the case of linearly rising loads. The limit of very fast loading corresponds to $k \to \infty$, whereupon $\alpha \to 0$ and $\eta \to 1$, since the first and third terms in Eq. (3.2.9c) become negligible. The disturbance then propagates at the bar wave speed in the matrix. Static loading is represented by the limit $k \to 0$ or $\alpha \to \infty$, for which the first two terms of Eq. (3.2.9c) become small and one has the asymptotic solution

$$\eta \to \frac{1}{2\alpha\beta} \qquad\qquad (3.2.12)$$

For this limit, substituting Eq. (3.2.12) into Eqs. (3.2.6a) and (3.2.11) yields

19

$$l_s \to \frac{1-f}{f}\frac{E_m R}{2\tau}\varepsilon \qquad\qquad (3.2.13a)$$

$$u \to u^{(st)} = \left(\frac{1-f}{f}\right)^2 \frac{E_m^2 R}{4E_f\tau}\varepsilon^2 \qquad\qquad (3.2.13b)$$

which coincide with the results obtained by McCartney [10].

Equations (3.2.10) and (3.2.13b) show that for loads that increase linearly with time, the form of the traction law is identical in the static and dynamic cases and

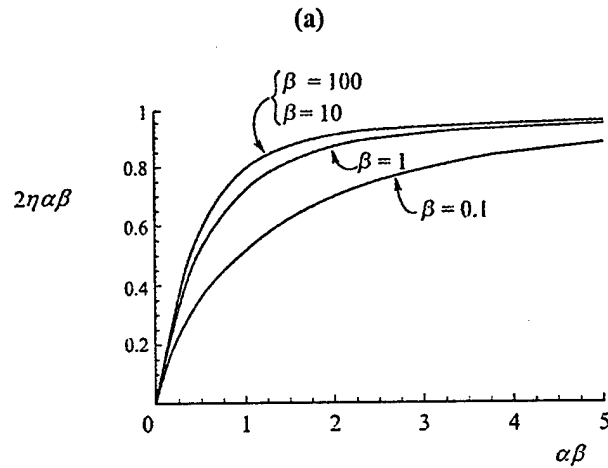$$\frac{u}{u^{(st)}} = 2\alpha\beta\eta \qquad . \qquad\qquad (3.2.14)$$

Thus the strength of the effects arising from inertia is measured by the degree to which the limit of Eq. (12) is not approached. This can be conveniently summarised by comparing the product $2\alpha\beta\eta$ to unity.

Large β. Asymptotic analysis of Eq. (3.2.9c) shows that in the limit $\beta \to \infty$, $2\alpha\beta\eta \to 2\left[\sqrt{(\alpha\beta)^4 + (\alpha\beta)^2} - (\alpha\beta)^2\right]$ (second, third, and fourth terms of Eq. (3.2.9c) dominant), which is a function of $\alpha\beta$ and not of β separately; and Fig. 3a shows that this limit is approached quite closely for $\beta > 1$, which is expected, for example, for composites containing relatively stiff fibres ($E_f > E_m$). Fig. 3a also suggests that, as an engineering estimate, inertial effects are large when
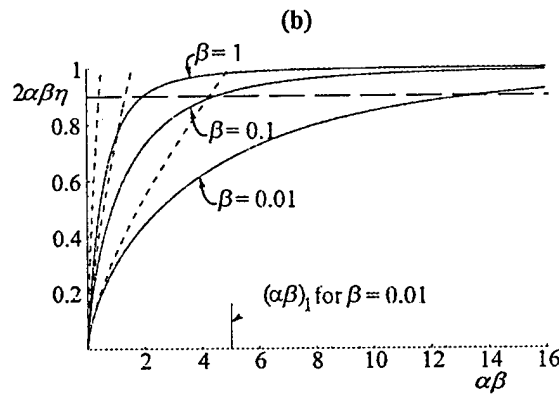
$$\alpha\beta \equiv \frac{f}{1-f}\frac{\tau}{Rk}\frac{c_m}{E_m} \leq 2 \qquad (\beta > 1) \qquad . \qquad (3.2.15)$$

Remembering that k^{-1} is the time constant of the loading, this condition can be rewritten

$$k^{-1} < 2\frac{1-f}{f}\frac{E_m}{\tau}\frac{R}{c_m} \qquad (\beta > 1) \qquad . \qquad (3.2.16)$$

20

(a)

(b)

Figure 3: The product $2\alpha\beta\eta$, which indicates the relative importance of inertial effects in the bridging phenomenon. (a) Numerical results for representative values of β. (b) Numerical results for $2\alpha\beta\eta$ compared with asymptotic limit for large E_m (dashed curves). The value of $(\alpha\beta)_1$ is marked for $\beta = 0.01$ and is to be compared with the value of $\alpha\beta$ at which $2\alpha\beta\eta \approx 0.9$, which is taken as a representative cutoff for significant inertial effects.

21

Small β. The limit of a relatively stiff matrix can be analysed by observing that $\alpha \propto E_m^{\frac{1}{2}}$ while β $\propto E_m^{-1}$; and that Eq. (3.2.9c) in the limit $E_m \to \infty$ therefore yields the limiting solution $\eta \to (2\alpha)^{-1/3}$ (first and last terms of Eq. (3.2.9c) dominant). Thus $2\alpha\beta\eta \to (2\alpha\beta)^{2/3}\beta^{1/3}$ when $\alpha\beta \to 0$. Figure 3b shows this approximation for three values of $\beta \le 1$. While the limit is approached only for $\alpha\beta$ so small that $2\alpha\beta\eta$ is also small, it can nevertheless be used as the basis for engineering estimates of the condition for significant inertial effects, i.e., the first significant departure of $2\alpha\beta\eta$ from unity. The construction of Fig. 3b suggests that inertial effects will be significant when $\alpha\beta < 4(\alpha\beta)_1$, where $(\alpha\beta)_1$ is the value of the product $\alpha\beta$ at which the equation $(2\alpha\beta)^{2/3}\beta^{1/3} = 1$ is satisfied; i.e.,

$$\alpha\beta < \frac{2}{\beta^2} \qquad (\beta < 1). \qquad (3.2.17)$$

This leads to the criterion for significant inertial effects for composites with relatively stiff matrices that

$$k^{-1} < 2 \left[\frac{1-f}{f}\right]^3 \frac{E_m^2}{E_f^2} \frac{E_m}{\tau} \frac{R}{c_m} \qquad (\beta < 1) \qquad . \qquad (3.2.18)$$

The criteria of Eqs. (3.2.16) and (3.2.18) coincide when $\beta = 1$. Since $2\alpha\beta\eta < 1$ always, inertial effects increase the stiffness, dp/du, of the traction law for loads that increase linearly in time.

Conclusion:

Some analytical results have been presented for the problem of bridging by the mechanism of fibre pullout when the inertia of the fibre and the matrix are taken into account. With this model, we also calculated simple criteria for significant inertial effects in the bridging mechanism in representative mode I crack propagation problems. We find that the inertial effects in the bridging mechanism will often be significant for a matrix crack propagating dynamically in the

22

steady state ACK limit in a brittle matrix continuous fibre composite or delamination in laminates reinforced by through-thickness stitching or rods.

We also find that significant inertial effects are favored by low fibre volume fraction, low friction stress, low matrix bar wave speed, and low fibre modulus; and high fibre diameter and high matrix modulus. If the fibre modulus is high enough (relative to the matrix modulus), the criterion for inertial effects becomes independent of fibre modulus. The matrix density enters the criterion only through the matrix bar wave speed. The criterion is always independent of the fibre density.

Finally, we also find that for pullout or bridging stresses that rise linearly in time, the instantaneous crack displacement is less in the presence of inertial effects than it would be under static loading to the same bridging stress. However, solutions for pullout from a rigid matrix suggest that, if the bridging stress rises rapidly and is then held at a constant value, the crack displacement when all particle motion finally stops will be greater than it would have been under static loading to that stress level. Thus regimes of both hardening and softening of the bridging traction law due to inertial effects can be expected in bridged crack problems.

We also formulated fast numerical solutions for general loading cases and hence have a scheme to compute the bridging law for fairly general conditions [4]. This will be required to solve large-scale bridging, dynamic crack problems to self-consistency (bridging tractions unknown *a priori*). The history dependent bridging law thus computed will form the basic ingredient in the computation of the structural response of the composite under dynamic loading conditions.

3.4 Mechanics of Crack Growth in Through-Thickness Reinforced DCB Specimens

In this portion of the research [5,6], the role of bridging by stitches or rods on steady state dynamic crack growth is analyzed. In particular, the dynamics of crack growth for through thickness reinforced double cantilever beam (DCB) specimens are examined. The DCB specimen is widely used in Mode I fracture toughness tests of polymers and composites. Certain solution characteristics as a result of the bridging are first identified. In the next section, we look into detail into the energetics of crack growth for a through thickness reinforced DCB specimen loaded by a flying wedge. The double cantilever beam (DCB) specimen loaded dynamically by a flying wedge offers a relatively simple experimental approach to analyzing the mode I dynamic delamination problem. The test is especially attractive for studying the bridging effects supplied by through-thickness reinforcement (e.g., stitches or rods) in laminates. The role of bridging by stitches or rods on steady state dynamic crack growth was computed by solving the bridged crack problem within the framework of beam theory.

Beam Theory Formulation and Solution Characteristics:

The equations of motion for the beam element are:

$$\frac{\partial N}{\partial x} = \rho\, b\, h\, \frac{\partial^2 u}{\partial t^2} \tag{3.4.1a}$$

$$\frac{\partial Q}{\partial x} - p(w,t)\, b = \rho\, b\, h\, \frac{\partial^2 w}{\partial t^2} \tag{3.4.1b}$$

$$\frac{\partial M}{\partial x} - Q = \rho\, I \frac{\partial^2 \phi}{\partial t^2} \tag{3.4.1c}$$

where u(x,t) and w(x,t) are the in-plane and transverse displacements of the neutral plane respectively, ϕ(x,t) is the clockwise rotation of the cross-section, t is the time variable, N is the axial force, Q is the shear force, M is the bending moment, 2h is the total thickness of the DCB specimen, b is the width of the specimen, ρ is the density, I (= $bh^3/12$) is the moment of inertia and p(w,t) is the

24

bridging traction corresponding to the opening mode. The time dependent bridging traction p corresponding to the opening mode is assumed to depend only on the transverse displacement w.

For a Timoshenko beam, the equations of motion for steady state cracking reduce to:

$$\frac{\partial^2 u}{\partial X^2} = 0 \tag{3.4.2a}$$

$$\frac{\partial^4 w}{\partial X^4} + \frac{c_l^2}{(R - c_l^2)(1 - c_l^2)} \frac{12\,R}{h^2} \frac{\partial^2 w}{\partial X^2}$$

$$- \frac{1}{(R - c_l^2)} \frac{1}{E\,h} \frac{\partial^2 p(w,X)}{\partial X^2} + \frac{1}{(R - c_l^2)(1 - c_l^2)} \frac{12\,R}{E\,h^3} p(w,X) = 0 \tag{3.4.2b}$$

$$\frac{\partial \phi}{\partial X} = \frac{p(w,X)}{R\,E\,h} - \frac{(R - c_l^2)}{R} \frac{\partial^2 w}{\partial X^2} \tag{3.4.2c}$$

where $X = x - v\,t$, $c_l^2 = \rho v^2 / E$ and $R = \kappa\,G/E$ and where v is the (constant) velocity of the crack tip. In the limit of steady state crack velocity $v \to 0$, we obtain the equations corresponding to the static case.

Similarly, it is easy to show that for and Euler-Bernoulli beam (where both the shear deformation and rotational inertia is ignored), equations of motion for steady state cracking reduce to:

$$\frac{\partial^2 u}{\partial X^2} = 0 \tag{3.4.3a}$$

$$\frac{\partial^4 w}{\partial X^4} + \frac{12\,c_l^2}{h^2} \frac{\partial^2 w}{\partial X^2} + \frac{12}{E\,h^3} p(w,X) = 0 \tag{3.4.3b}$$

where $X = x - v\,t$, v is the (constant) velocity of the crack tip, $c_l^2 = \rho v^2 / E$ and $R = \kappa\,G/E$. We shall now consider a linear bridging law of the following type:

$$p(w,X) = p_0 + \beta_3 w \tag{3.4.4}$$

A linear bridging law of the type above is a simple but realistic constitutive law. In the results that follow, we non-dimensionalize the length variables by the laminate thickness h. Therefore, $w \equiv h\,W$, $u \equiv h\,U$ and $X \equiv h\,\xi$. We now analyze the solution characteristics.

25

For a linear bridging law in Equation 3.4.4, $U(\xi)=0$. The transverse displacement obeys:

$$\frac{\partial^4 W}{\partial \xi^4} + \beta^2 \frac{\partial^2 W}{\partial \xi^2} + b^2 W + d^2 = 0 \tag{3.4.5a}$$

Also, for the Timoshenko beam the clockwise rotation ϕ is:

$$\frac{\partial \phi}{\partial \xi} = \frac{(p_0 + \beta_3 hW)}{RE} - \frac{(R - c_i^2)}{R}\frac{\partial^2 W}{\partial \xi^2} \tag{3.4.5b}$$

The coefficients β, b and d in Equation 3.4.5a are:

For Timoshenko beam:

$$\beta = \sqrt{\frac{12\, c_i^2\, R}{(1 - c_i^2)(R - c_i^2)} - \frac{\beta_3 h}{(R - c_i^2)E}}$$

$$b = \sqrt{\frac{R}{(1 - c_i^2)(R - c_i^2)}\frac{12\beta_3 h}{E}}$$

$$d = \sqrt{\frac{R}{(1 - c_i^2)(R - c_i^2)}\frac{12 p_0}{E}} \tag{3.4.6a}$$

For Euler-Bernoulli (E-B) beam:

$$\beta = \sqrt{12 c_i^2}\;; \qquad b = \sqrt{\frac{12\beta_3 h}{E}}\;; \qquad d = \sqrt{\frac{12 p_0}{E}}\;; \tag{3.4.6b}$$

and where $c_i^2 = \rho v^2 / E$, $c_s^2 = \rho v^2 /(\kappa G)$ and $R = \kappa G / E$. In the limit that the crack velocity approaches zero ($v = c_i = c_s \to 0$), we retrieve the static case of Roberta and Cox [17,18].

The general solution to equation 3.4.5a is:

$$W(\xi) = -\frac{d^2}{b^2} + K_1 e^{-\sqrt{-\frac{\beta^2}{2} - \frac{1}{2}\sqrt{\beta^4 - 4b^2}}\,\xi} + K_2 e^{+\sqrt{-\frac{\beta^2}{2} - \frac{1}{2}\sqrt{\beta^4 - 4b^2}}\,\xi}$$

$$+ K_3 e^{-\sqrt{-\frac{\beta^2}{2} + \frac{1}{2}\sqrt{\beta^4 - 4b^2}}\,\xi} + K_4 e^{+\sqrt{-\frac{\beta^2}{2} + \frac{1}{2}\sqrt{\beta^4 - 4b^2}}\,\xi} \tag{3.4.7}$$

There are three regimes to the solution behavior and these are identified below. In the equations below, we have introduced the dimensionless quantities:

$$S = \frac{\beta_3 h}{12 \kappa G} \quad \text{and} \quad R = \frac{\kappa G}{E}$$

- Case 1: $\beta^2 < 0$ and $\beta^4 > 4b^2$ => Exponential behavior

  - For Timoshenko beam, this is true provided:

$$\frac{\rho v^2}{E} \leq \frac{S}{1+S} \quad \text{and} \quad 3\,(S(1-c_I^2)-c_I^2)^2 \geq S(1-c_I^2)(R-c_I^2) \tag{3.4.8a}$$

  - For the E-B beam, the above condition is never satisified.

- Case 2: $\beta^2 > 0$ and $\beta^4 > 4b^2$ => Oscillatory and non-decaying behavior

  - For Timoshenko beam, this is true provided:

$$\frac{\rho v^2}{E} > \frac{S}{1+S} \quad \text{and} \quad 3\,(S(1-c_I^2)-c_I^2)^2 \geq S(1-c_I^2)(R-c_I^2) \tag{3.4.8b.1}$$

  - For the E-B beam, this condition is satisified when:

$$\frac{\rho v^2}{E} \geq 2\sqrt{S R} \tag{3.4.8b.2}$$

- Case 3: $\beta^4 < 4b^2$ => Oscillatory with exponential decay behavior

  - For the Timoshenko beam, this is true when:

$$3\,(S(1-c_I^2)-c_I^2)^2 < S(1-c_I^2)(R-c_I^2) \tag{3.4.8c.1}$$

  - For the E-B beam, this is true when:

$$\frac{\rho v^2}{E} < 2\sqrt{S R} \tag{3.4.8c.2}$$

The arbitrary constants K_1, K_2, K_3, and K_4 in Equation 15 are defined through the associated boundary and continuity conditions. The conditions determined above give us insight into when dynamic effects can significantly alter the mechanisms of deformation and the resultant bridging phenomena. For instance, if the crack tip velocity exceeds the conditions prescribed in either

(3.4.8a), oscillatory displacement fields will be introduced in the wake of the crack. These multiple oscillations are of a very different form to the crack face interpenetration caused sometimes by bridging effects in the static case. When such oscillations result from dynamic effects, the mechanics of bridging and the efficacy of through thickness bridging ligaments on the energetics of crack growth will be considerably altered. For example, stick-slip propagation modes become likely.

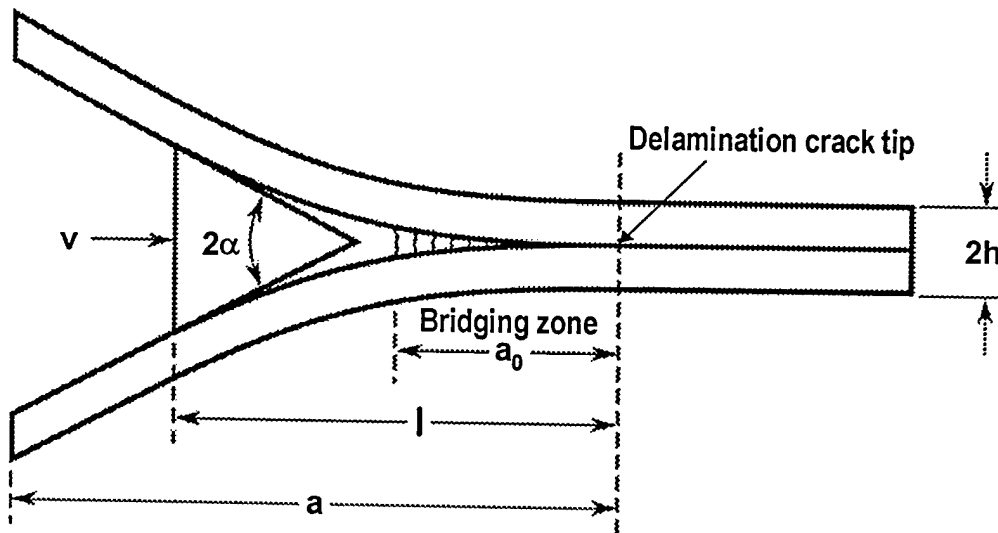### Wedge-Loaded Double Cantilever Beam

Figure 4: Schematic of through-thickness reinforced DCB specimen loaded with a flying wedge

We now concentrate on the mechanics of delamination for the Euler Bernoulli beam, where both shear deformation and rotational inertia can be ignored. Therefore the constants β, b and d referred to hereafter are the ones presented in Eqn. 3.4.6b. The double cantilever beam (DCB) specimen loaded dynamically by a flying wedge, of constant velocity, offers a relatively simple experimental approach to studying the mode I dynamic delamination problem (Fig. 4). The test is especially attractive for studying the bridging effects supplied by through-thickness reinforcement (e.g., stitches or rods) in laminates. In figure 4, 2α is the wedge angle, l is the distance between the wedge and the crack tip and a_0 is the length of the bridging zone. In non-dimensional form, $l \equiv h L$, and $a_0 \equiv h A_0$. Due to symmetry, we focus our attention only on the

28

top half of the DCB specimen. A detailed analysis of the role of the bridging on dynamic delamination behavior is presented in this section. The analysis is valid when the bridging constituent has a linear bridging relationship (as presented in Eqn. 3.4.4).

For the unbridged portion, the deflection profile ($w_u \equiv h\,W_u$) is obtained by setting b = d = 0. Therefore:

$$\frac{\partial^4 W_u}{\partial \xi^4} + \beta^2\, \frac{\partial^2 W_u}{\partial \xi^2} = 0 \qquad\qquad \text{for } (-L \leq \xi \leq -A_0) \qquad (3.4.9a)$$

$$\frac{\partial^4 W}{\partial \xi^4} + \beta^2\, \frac{\partial^2 W}{\partial \xi^2} + b^2 W + d^2 = 0 \qquad \text{for } (-A_0 < \xi \leq 0) \qquad (3.4.9b)$$

The relevant boundary conditions are:

$$W(\xi = 0) = 0, \qquad\qquad W'(\xi = 0) = 0,$$

$$W_u'(\xi = -L) = -\alpha, \qquad\qquad W_u''(\xi = -L) = 0 \qquad . \qquad (3.4.10)$$

The deflection profiles should satisfy the continuity conditions at the end of the bridging zone ($\xi = -A_0$). The continuity conditions are:

$$W(\xi = -A_0) = W_u(\xi = -A_0), \qquad W'(\xi = -A_0) = W_u'(\xi = -A_0),$$

$$W''(\xi = -A_0) = W_u''(\xi = -A_0), \qquad W'''(\xi = -A_0) = W_u'''(\xi = -A_0) \qquad . \qquad (3.4.11)$$

The governing equation (3.4.9) together with the boundary conditions (3.4.10) and the continuity conditions (3.4.11) will completely determine the deflection profile of the beam. The bridging zone length (A_0) will be dictated by the critical crack opening displacement ($w_c \equiv h\,W_c$) required for failure of the bridging ligament. Therefore, A_0 is obtained by solving:

$$W(\xi = -A_0) = W_c \qquad . \qquad (3.4.12)$$

The energy release rate (G_{Total}), determined through the total energy balance is:

$$G_{Total} = \frac{1}{B}\left(\frac{\partial U_{ext}}{\partial a} - \frac{\partial U_s}{\partial a} - \frac{\partial U_k}{\partial a} \right) \qquad (3.4.13)$$

where U_{ext} is the work done by the applied load, U_s is the strain energy, U_k is the kinetic energy, B is the uniform width of the DCB specimen, and a is the crack length. For steady state crack extension a = v t, where v is the crack velocity and t is time. Further, under steady state

delamination, there is no net change in strain energy ($U_s = 0$) upon crack extension since both the material ahead of the crack tip and the material in the wake of the wedge have zero strain energy. However, for small α:

$$\frac{\partial U_k}{\partial t} = 2\frac{\partial}{\partial t}\left(\frac{1}{2}m\,v_n^2\right) = B\rho h v^3 Sin^2(\alpha) \approx B\rho h v^3 \alpha^2 \qquad (3.4.14a)$$

$$\frac{\partial U_{ext}}{\partial t} = 2\,.\text{Applied Force}.\,v$$

$$= -2\,Sin(\alpha)\,v\,Q\big|_{\xi=-L} \approx Bv\frac{\alpha E h}{6}\frac{\partial^3 W_u}{\partial\xi^3}\bigg|_{\xi=-L} \qquad (3.4.14b)$$

where m is the mass in the wake behind the wedge, v_n is the normal velocity and Q is the shear force in the beam. Therefore,

$$G_{Total} = \frac{\alpha E h}{6}\frac{\partial^3 W_u}{\partial\xi^3}\bigg|_{\xi=-L} - \rho h v^2 \alpha^2 \qquad (3.4.15)$$

In addition, by application of the dynamic J-integral, the energy released at the crack tip is related to the bending moment M by :

$$G_{Tip} = \frac{12}{Eh^3}\left[M_{\xi=0}\right]^2 = \frac{Eh}{12}\left(\frac{\partial^2 W}{\partial\xi^2}\bigg|_{\xi=0}\right)^2 \qquad (3.4.16)$$

In general, due to crack bridging, $\Delta G = G_{Total} - G_{Tip} \neq 0$. The energy difference, ΔG, is the extra work done in fracturing the bridging ligaments. In the absence of crack bridging, $\Delta G = 0$ and $G_{Total} = G_{Tip} = G_0$ is given by:

$$G_0 = \frac{\rho h v^2 \alpha^2}{Tan^2(\lambda/2)} \qquad (3.4.17)$$

With this formalism, detailed calculations of the deflection profile and crack energy release rate was computed for the linear bridging law [5]. Analytical results were obtained for steady state crack propagation conditions. The key results are summarized below:

- The magnitude of the bridging traction, which is controlled by the properties of the through thickness reinforcement, plays a significant role in the crack growth behavior. For steady

state crack growth conditions, different regimes of the solution behavior have been identified which would correspond to different crack propagation characteristics. Critical velocities that demarcate the various solution regimes have been identified.

- Steady state crack growth is attainable for this loading configuration provided certain conditions are satisfied. Regions of stable crack growth as a function of the material properties of the through thickness reinforcement, the size of the DCB specimen and the velocity of the wedge have been identified. This provides guidelines for design of experiments to probe the efficacy of bridging on improving the dynamic fracture toughness of through thickness reinforced structures.

3.5 Dynamic Crack Energy Release Rate for Orthotropic Laminates

In this portion of the work, we compute explicit relations for the dynamic crack energy release rate and crack tip stress intensity factors in a form most amenable to computational work for a crack propagating along any principal axis in an orthotropic material [6]. The results presented in this form may be particularly useful for work on delamination cracks in laminated composites, which are orthotropic in many important applications. Although Yang and co-workers [13] presented results for a mixed mode crack in an orthotropic material, it is in a form that is not best suited for immediate computation. By an adaptation of the Stroh method of analysis used by Wu [14], the results of Yang et al. [13] are rendered here in a different form better suited to numerical evaluation. The role of orthotropic anisotropy in determining the velocity dependence of G_d is then illustrated for delamination cracks in typical ceramic, metal and polymer matrix laminated composites.

The relation between the energy release rate and the crack tip stress intensity factor is central to fracture analysis. It appears, for example, in the derivation of stress intensity factors from applications of the J-integral and in the derivation via energy arguments of integral equations for bridged cracks from weight functions. Freund [15] showed that the dynamic crack energy release rate for an extending crack in an elastic body can be written as the modified J-integral, which leads to the G-k relationship in the following, convenient form:

$$G_d = \frac{1}{2} k^D(t)^T L^{-1} k(t)$$

where G_d is the dynamic crack energy release rate and $k(t)$ is the instantaneous crack tip stress intensity factors (see Eq. 4.19 in Wu [14] and references therein). The elements of the L^{-1} matrix are universal functions, in the sense that they are independent of the details of the applied loading or on the configuration of the body being analyzed. We calculated the L^{-1} matrix when the material possesses orthotropic symmetry and when the crack is extending along one of the principal axis [6]. In this case, the off-diagonal elements of the matrix are zero and the diagonal elements of the L^{-1} matrix is just dependent on the elastic properties of the orthotropic medium and the instantaneous value of the crack tip velocity. For an orthotropic material with the crack propagating along the 1 direction (and direction 3 being the plane strain direction), elements of the L^{-1} matrix are:

$$L^{-1} = \frac{1}{C_{66}} \begin{pmatrix} \dfrac{-(\gamma_5 + \gamma_1 \gamma_4)}{(\gamma_4^2 - \gamma_3 \gamma_5)} & 0 & 0 \\ 0 & \dfrac{-(\gamma_3 - \gamma_2 \gamma_4)}{(\gamma_4^2 - \gamma_3 \gamma_5)} & 0 \\ 0 & 0 & \dfrac{1}{\gamma_6} \end{pmatrix}$$

where the γ's are presented in detail in the appendix paper [6]. We can also define the generalized Rayleigh wave function $R(v)$ as

$$R(v) = \gamma_4^2 - \gamma_3 \gamma_5$$

and the Rayleigh wave speed (v_r) is obtained by setting $R(v_r) = 0$.

The diagonal elements $L^{-1}_{1,1}$ and $L^{-1}_{2,2}$ were computed numerically for cracks propagating along different principal axes in various representative composites. The L^{-1} matrix elements are functions of the elastic properties and the instantaneous crack velocity. Each diagonal element approaches the corresponding static value as $v \to 0$ and has the property of $O[(v_r - v)^{-1}]$ as $v \to v_r$, where v_r is the Rayleigh wave speed. In addition, we find that the that the variation in the normalized crack energy release rate ($L^{-1} / [L^{-1}]_{static}$) as a function of the normalized crack

32

velocity v/v_r can be rationalized in terms of the orthotropy parameters λ and ρ (Suo et al.,[16]). For the same normalized crack speed, the normalized mode I contribution ($L^{-1}_{1,1}$ / $[L^{-1}_{1,1}]_{static}$) to the dynamic crack energy release rate increases as λ monotonically increases and as ρ monotonically decreases. For the same normalized crack speed, the normalized mode II contribution ($L^{-1}_{2,2}$ / $[L^{-1}_{2,2}]_{static}$) to the dynamic crack energy release rate increases as λ increases and as ρ decreases. However, as opposed to the mode I case, the variation on λ and ρ is much smaller. In addition, we observe that although the energy release rate shows a monotonic dependence on λ, the dependence on ρ, for small ρ, is not monotonic.

To conclude, we have provided an analytical form for easy estimation of the dynamic crack energy release rate, in terms of the crack tip stress intensity factors, has been presented for cracks propagating along any of the principal axis in orthotropic material systems. The dynamic crack energy release rate depends on the magnitude of the two orthotropic parameters and the instantaneous crack tip velocity. The dynamic crack energy release rate is $O[(v_r - v)^{-1}]$ as $v \to v_r$, and where v_r is the Rayleigh wave speed. The variation in the dynamic crack energy relase rate for orthotropic materials can be rationalized in terms of the two orthotropy parameters λ and ρ.

4. REFERENCES INCLUDING PAPERS PREPARED UNDER THIS CONTRACT

1.* B.N.Cox and N.Sridhar, "A Traction Law for Fiber Tows Bridging Mixed Mode Cracks", in preparation for submission to *Composites*, Feb. 2001

2.** B.N.Cox, N.Sridhar, and I.J.Beyerlein, "Inertial effects in the Pullout Mechanism during Dynamic Loading of a Bridged Crack", submitted to *Journal of Mechanics and Physics of Solids*, June 2000

3.* N.Sridhar, B.N.Cox, I.J.Beyerlein, and C.L.Dunn, "Mechanics of Crack bridging under dynamic loads", submitted to *MRS Fall Meeting*, Boston, December 2000

4.* N.Sridhar, B.N.Cox and C.L.Dunn, "Inertial effects in the Pullout Mechanism of a Bridged Crack – Numerical Solutions for Generalized loads ", in preparation for submission to *Journal of Applied Mechanics*, March 2001

5.* N.Sridhar, B.N.Cox, I.J.Beyerlein, and Roberta Massabò, "Delamination mechanics in Through-Thickness Reinforced Structures under dynamic crack growth conditions", in preparation for submission to *Journal of Mechanics and Physics of Solids*, Feb. 2001

6.** N.Sridhar, B.N.Cox, I.J.Beyerlein and R. Massabò "Dynamic Delamination in Through-Thickness reinforced DCB specimens", submitted to *Intl. Congress on Fracture*, (Hawaii, December 2001), Jan. 2001

7.** N.Sridhar, I.J.Beyerlein and B.N.Cox, "Computation of Dynamic Crack Energy Release Rate for Orthotropic Systems," in preparation for submission as a "brief note" to *Journal of Applied Mechanics*, February 2001

8.** R. Massabo and B. N. Cox, "Beam Theory and Weight Function Methods for Mode I Delamination with Large Scale Bridging," *Proc. Int. Conf. on Fracture, ICF10, Hawaii, Dec. 2001.*

9. D. B. Marshall, B. N. Cox and A. G. Evans, "The Mechanics of Matrix Cracking in Brittle-Matrix Fiber Composites," *Acta Metall.* **33**, 2013-2021 (1985).

10. L. N. McCartney, "Mechanics of Matrix Cracking in Brittle-Matrix Fibre-Reinforced Composites," *Proc. Roy. Lond.* **A409**, 329-350 (1987).

11. J. W. Hutchinson and H. M. Jensen, "Models of Fiber Debonding and Pullout in Brittle Composites with Friction," *Mechanics of Materials*, **9**, 139-163 (1990).

12. J. D. Achenbach, *Wave Propagation in Elastic Solids*, North-Holland, 1973, pp. 138-143.

13.   Yang, W., Suo, Z., and Shih, C.F., 1991, "Mechanics of dynamic debonding", *Proc. R. Soc. Lond. A*, vol. 433, 679-697

14.   Wu, K.-C., 1989, "On the crack tip fields of a dynamically propagating crack in an anisotropic solid", *Intl. Journal of Fracture*, vol. 41, 253-266

15.   Freund, L.B., 1972, "Energy flux into the tip of an extending crack in an elastic solid", *Journal of Elasticity*, vol. 2, 341-349

16.   Suo, Z., Bao, G., Fan, B., and Wang,T.C., 1991, "Orthotropy Rescaling and Implications for Fracture in Composites", *Int. J. Solids. Structures*, vol.28, 235-248

17.   R. Massabò and B. N. Cox, "Concepts for Bridged Mode II Delamination Cracks," *J. Mech. Phys. Solids*, **47**, 1265-1300 (1999).

18.   R. Massabò and B. N. Cox, "Unusual Characteristics of Mixed Mode Delamination Fracture in the Presence of Large Scale Bridging," *Mechanics of Comp. Mater. and Struct.*, in press.

19.   B. N. Cox, "Extrinsic Factors in the Mechanics of Bridged Cracks," *Acta Metallurgica et Materialia* **39**, 1189-1201 (1991).

20.   B. N. Cox and D. B. Marshall, "Stable and Unstable Solutions for Bridged Cracks in Various Specimens," *Acta Metall. et Mater.* **39**, 579-89 (1991).

21.   B. N. Cox and D. B. Marshall, "Concepts for Bridged Cracks in Fracture and Fatigue," Overview No. 111, *Acta Metall. Mater.* **42**, 341-63 (1994).

22.   D. B. Marshall and B. N. Cox, "A J-Integral Method for Calculating Steady-State Matrix Cracking in Composites," *Mechanics of Materials* **7**, 127-33 (1988).

** Drafts appended to report

* Prepared under this contract

5. COLLABORATIONS

We continue to collaborate with Dr. Irene Beyerlein of Los Alamos National Labs and Dr. Roberta Massabò of University of Genova, Italy on modeling the mechanisms of deformation under dynamic loads.

Prof. Ares Rosakis of Caltech, with a sub-contract under this program (~$20K), is conducting experiments for detailed study of the dynamic fiber pull-out / push-in process to provide data with which the validity of the pull-out model will be assessed. Through the use of a carefully designed 2D model material system and high-speed diagnostics, a complete quantitative description of process can be obtained which makes direct comparison with the theoretical model possible.

6. FINANCIAL SUMMMARY

As of January 21, 2001, we had received $188k in total funding since the inception of the program (Sept 2, 1999), of which approximately $35k stands unspent. Thus we are spending at slightly below linear rate. We expect the activity and the spending level in the program to increase over the next two months.

We continue to add substantial value to our contract through collaborations with Dr. Irene Beyerlein of Los Alamos National Labs and Dr. Roberta Massabò of the University of Genova, Italy. The only expenses incurred in these collaborations so far have been for the travel expenses of Dr. Beyerlein and Dr. Massabò to Rockwell Science Center. Dr. Beyerlein visited us 2 times in this reporting period (~ a week per visit) and the total travel costs incurred were $1500. Dr. Massabò visited us 2 times in this reporting period (~ a week per visit) and the total travel costs incurred were $2000.

7. SCIENTIFIC PERSONNEL SUPPORTED BY GRANT

Dr. Sridhar Narayanaswamy, Member of the Technical Staff,
Design and Reliability Department, Materials Science Function
Rockwell Science Center

Dr. Brian Cox, Principal Scientist, Materials Science Function
Rockwell Science Center

Ms. Catherine Dunn, junior in the Department of Aeronautics, MIT was supported as a summer intern (May – July 2000) under the ARO grant.

NOTE: Not included for internal distribution

8. APPENDIX

We append drafts of the following four papers:

1. B.N.Cox, N.Sridhar, and I.J.Beyerlein, "Inertial effects in the Pullout Mechanism during Dynamic Loading of a Bridged Crack", submitted to *Journal of Mechanics and Physics of Solids*, June 2000

2. N.Sridhar, I.J.Beyerlein and B.N.Cox, "Computation of Dynamic Crack Energy Release Rate for Orthotropic Systems," in preparation for submission as a "brief note" to *Journal of Applied Mechanics*, February 2001

3. N.Sridhar, I.J.Beyerlein, B.N.Cox, and R. Massabò, "Dynamic Delamination in Through-Thickness reinforced DCB specimens", submitted to *Proc. Int. Conf. on Fracture, ICF10, Hawaii, Dec. 2001.*

4. R. Massabò and B. N. Cox, "Beam Theory and Weight Function Methods for Mode I Delamination with Large Scale Bridging," submitted to *Proc. Int. Conf. on Fracture, ICF10, Hawaii, Dec. 2001.*

INERTIAL EFFECTS IN THE PULLOUT MECHANISM DURING DYNAMIC LOADING OF A BRIDGED CRACK

B. N. Cox and N. Sridhar
Rockwell Science Center
1049 Camino Dos Rios
Thousand Oaks, CA 91360
U.S.A.

and

I. Beyerlein
Los Alamos National Laboratory
Los Alamos, New Mexico
U.S.A.

ABSTRACT

Inertial effects in the mechanism of fibre pullout during the dynamic propagation of a bridged crack are examined by reposing simple shear lag models of pullout as problems of dynamic wave propagation. The only coupling considered between the fibres and the matrix is uniform, rate independent friction – no debond energy is included. Analytical solutions are found to the problem of the coupled waves in the fibres and the matrix that propagate away from the fracture plane of the bridged crack as the bridging tractions increase with time. These solutions yield the time-dependent relationship between the crack opening displacement and the bridging traction. Engineering criteria for inertial effects being significant are deduced by comparing the dynamic bridging traction law with its counterpart for static loading, which is recovered as a limit of the dynamic case. The criteria are evaluated for two crack cases: the asymptotic limit of a long, fully bridged matrix crack propagating unstably through a fibrous composite under remote tension; and a delamination crack bridged by stitches or rods that is loaded by a flying wedge splitting a double cantilever beam. In both cases, the rate of increase of the crack opening displacement appears to be sufficient for inertial effects to be pronounced in the bridging (pullout) mechanism. Expected trends of the significance of inertial effects with material and geometrical parameters are identified.

1.   Introduction

The pullout mechanism is the fundamental source of toughening and fracture resistance in many composites.   In brittle matrix composites, reinforcing fibres that are weakly bonded to the matrix can survive the passage of matrix cracks, across which they then provide bridging tractions that shield the crack tip from the applied load. The main mechanism of load transfer from the fibres to the matrix is interfacial friction.   In polymeric laminates reinforced through the thickness by stitches or rods, analogous pullout phenomena are observed, but on the scale of fibre tows, which may be 1 mm in diameter, rather than on the scale of individual fibres (10 − 100 μm).   Scale considerations aside, the mechanics of pullout are very similar in the two cases. Other systems in which bridging entities are coupled to a matrix by friction include so-called self-reinforced polycrystalline ceramics, in which elongated grains bridge cracks; and ceramic layered systems, in which fractured layers slide past one another during failure.

For mode I cracks, the shielding effect created by the pullout phenomenon can be summarised by a bridging traction law that relates the stress in the bridging entities at the fracture plane, T, to the crack opening displacement, $2u$. To a very good approximation in many cases, the tractions in the bridging entities can be replaced by an equivalent continuous traction, p, that is to be applied to the entire bridged interval of the fracture surfaces (e.g., Cox and Marshall, 1994). Predicting the traction law, $p(u)$, becomes one of the central problems of crack bridging theory.

The mechanics of pullout and the resulting traction law have been much studied and are well understood for static loading. Simple analytical forms are available for $p(u)$ when the frictional coupling of the reinforcement to the matrix is uniform and slip extends over distances that are large compared to the reinforcement diameter (Marshall, Cox, and Evans, 1985; McCartney, 1987). In this limit, which is a common case in ceramic composites and textile polymeric composites, the shear lag model of load transfer between the reinforcement and the matrix is accurate. Simple extensions of models of this class are also available to deal with small but nonzero levels of the work required to debond the reinforcement from the matrix prior to slip (Hutchinson and Jensen, 1990).

Given the relationship, $p(u)$, the characteristics of crack propagation can be computed by solving a bridged crack problem. In composites in which the bridging mechanism is most effective, the zone of bridging can be comparable to the crack length and much larger than features such as notches (Bao and Suo, 1992; Cox and Marshall, 1994) or, in the case of delamination cracks, the laminate thickness (Jain and Mai, 1995; Massabò and Cox, 1999). Crack propagation then does not follow Linear Elastic Fracture Mechanics, in the sense that there is no single material parameter such as toughness that correlates with the crack growth. Instead, the bridged crack problem is one of large scale bridging and the characteristics of propagation show features peculiar to the form of the traction law, $p(u)$ [Cox, 1991].

This paper extends existing models of the mechanics of pullout to high loading rates. An approach to evaluating a traction law that takes account of the inertia of the reinforcement

42

and the matrix is formulated as a direct extension of the elementary static loading model of McCartney (1987) and Marshall, Cox, and Evans (1985). The chosen base model for static loading has proven consistent with experiments in many material systems and has been the foundation of major advances in understanding damage in composites. The spirit of the present work is to seek equivalent insight into dynamic damage by incorporating the influence of inertia into the simplest credible model. Thus not all aspects of the micromechanics of pullout that could be important in some cases will be addressed. Instead, attention will be focused on identifying a characteristic time for the frictional pullout problem that will allow rapid assessment of when inertial effects will be important.

2. Idealisation of the Bridged Crack problem

The crack propagation and pullout problems are depicted schematically in Fig. 1a. A matrix crack propagates on the plane $z = 0$ and is bridged by intact fibres in its wake. (For simplicity of expression, the term fibre from here on will be used to refer to bridging entities of any kind, including stitches, rods, and bridging grains.) Upon the passing of the crack tip, a debond crack propagates along the length of each fibre away from the fracture plane. Propagation of the debond crack is governed by the fracture energy associated with the separation of the matrix and the fibre at the debond crack tip and the work done against friction in displacing the debonded fibre along its axis. In many composites, the debond energy is small and pullout is dominated by friction over much of the range of pullout displacements. Therefore, in this first model the debond energy will be ignored.

For static loading, the crack propagation problem can be idealised by replacing the process zone by elastic composite material down to the fracture plane and representing the phenomena within the process zone by bridging tractions applied continuously on the fracture surfaces (Fig. 1b). The bridging tractions, p, are related to the axial stress, T, in the fibres at the fracture plane by $p = fT$, where f is the area fraction of the fibres on the plane $z = 0$. For aligned continuous reinforcement, f is also the volume fraction of the fibres. The total crack opening displacement, $2u$, in the idealisation should be defined as the difference in the actual displacement evaluated across the process zone and the displacement that would be expected if the material in the process zone was elastic.

The traction law, $p(u)$, is derived by considering the micromechanics of the phenomena occurring within the process zone, which is to say the micromechanics of frictional sliding. The micromechanical problem can be represented by a small volume of material, e.g., the material bounded by one of the dotted rectangles in Fig. 1a. The traction boundary conditions for the representative volume are as follows. At $z = 0$, the matrix is traction-free, while the fibres sustain the axial traction T. At $z = l_s$, the strain in the fibres and the matrix must equal the average strain in the composite adjacent to the process zone ($z > l_s$). Shear tractions may arise along the vertical boundaries of the representative volume (parallel to z), but these are neglected.

In the problem of a crack propagating under static loading, the traction at $z = l_s$ for the representative volume associated with a fixed volume of material is assumed to rise from zero when the material is immediately behind the crack tip to increasing values as the material passes further back into the wake (Marshall et al., 1985). The tractions are not truly zero right at the crack tip, since the fibres are not stress-free, but assuming they are leads to reasonable results for the bridged crack problem as long as the fibres remain intact over sufficiently long distances into the crack wake. Then shielding of the crack tip is dominated by the bridging tractions acting in the further crack wake, where the boundary conditions are correct.

Further details of the analysis of the micromechanical problem may be found in McCartney (1987) and the appendix to Marshall et al. (1985).

In dynamic loading, the boundary conditions at the boundary of the process zone involve displacement and displacement rates as well as stress or strain conditions.

3. The Micromechanics of Dynamic Pullout

When friction is the only active force of resistance, the static pullout problem reduces to an idealization in which fibers are pulled out of a half-space to which they are not initially bonded. The dynamic problem is one of wave propagation along a fibre in the presence of frictional retardation and with no debond crack tip or crack tip field to be considered.

The archetypal problem is illustrated in Fig. 2. A representative volume consists of cylindrical fibres of radius R and volume fraction f embedded in a matrix ($z \geq 0$). The fibre and the matrix have axial Young's moduli E_f and E_m and densities ρ_f and ρ_m respectively. The axial displacement, strain, and stress of the fibre and the matrix are denoted u_f and u_m, ε_f and ε_m, and σ_f and σ_m, respectively. The axial displacements will be assumed to be the only nonzero displacement components induced by loading and to be uniform across any section of the fibre or the matrix. Thus the displacement, strain, and stress in the fibre and the matrix are functions of z and t only. These are the usual assumptions of shear lag theory with the simplest conditions of elasticity (Poisson's effect omitted). They are consistent with assuming that the friction forces are constant (unaffected by fibre contraction or dilation due to axial stresses).

There is no initial bond between the fibres and the matrix. The fibres are coupled to the matrix by friction tractions, τ_f, which are assigned the following properties. If relative motion exists between the fibres and the matrix, then

$$\tau_f = \tau \qquad (\dot{u}_f < \dot{u}_m) \qquad (1a)$$

$$\tau_f = -\tau \qquad (\dot{u}_f > \dot{u}_m) \qquad (1b)$$

where a dot indicates time differentiation, τ is a positive constant and $\tau_f > 0$ indicates friction tractions acting on the fibres in the positive z direction. When the fibres and the matrix are not in relative motion, the friction tractions may support stress gradients in the fibres and the matrix, provided that the required magnitude of τ_f does not exceed τ. Thus, by equilibrium considerations,

$$\left| \frac{\partial \sigma_f}{\partial z} - \rho_f \frac{\partial \dot{u}_f}{\partial t} \right| \le \frac{2\tau}{R} \quad \& \quad \left| \frac{\partial \sigma_m}{\partial z} - \rho_m \frac{\partial \dot{u}_m}{\partial t} \right| \le \frac{2f}{1-f} \frac{\tau}{R} \quad (\dot{u}_f = \dot{u}_m). \quad (1c)$$

Here the possibility is included that the matrix and the fibres have the same non-zero velocity and may also be accelerating together, although such general solutions will not be exhibited in this paper. With such a friction law, the dynamic wave equations describing those parts of the fibres and the matrix that are in relative motion may be written approximately as

$$\frac{\partial^2 u_f}{\partial z^2} = -\frac{2\theta\tau}{RE_f} + \frac{1}{c_f^2} \frac{\partial^2 u_f}{\partial t^2} \qquad (2a)$$

and

$$\frac{\partial^2 u_m}{\partial z^2} = \frac{2f}{1-f} \frac{\theta\tau}{RE_m} + \frac{1}{c_m^2} \frac{\partial^2 u_m}{\partial t^2} \qquad (2b)$$

where $\theta = 1$ if $\dot{u}_m > \dot{u}_f$ and $\theta = -1$ otherwise; and c_f and c_m are the bar wave velocities in the fibres and the matrix, given by

$$c_f = \sqrt{\frac{E_f}{\rho_f}} \qquad \& \qquad c_m = \sqrt{\frac{E_m}{\rho_m}} \quad . \qquad (2c)$$

The approximation of using the bar wave velocities rather than the longitudinal wave velocities in the z direction in the wave equations is consistent with the simplified treatment of stresses and strains and the assumed uniformity of the friction stress.

Boundary conditions in the dynamic case are as follows. At the fracture plane,

$$u_f(0, t) = 0 \qquad \& \qquad \sigma_m(0, t) = 0 \qquad (z = 0). \qquad (3)$$

At the boundary of the process zone (limit of relative fibre/matrix motion),

$$u_f = u_m = u_c \qquad\qquad (z = l_s) \qquad (4)$$

where u_c is the displacement of the adjacent intact composite; and conditions also exist on stress or strain and particle velocities. These further conditions depend on the nature of the loading history, which can be expressed as the function $\varepsilon(t)$, where ε is the strain in the z direction in the intact composite adjacent to the process zone boundary. The bridging traction, p, is related to ε by

$$p = \varepsilon E \tag{5a}$$

where the composite modulus, E, is given by

$$E = f E_f + (1 - f) E_m \qquad . \tag{5b}$$

In the depiction of Fig. 1a, the process zone boundary will propagate away from the fracture plane as $\varepsilon(t)$ rises. In the case to be considered in this paper, $\varepsilon(t)$ will be assumed to rise continuously and monotonically from zero. Placing the origin of time, $t = 0$, at the onset of nonzero $\varepsilon(t)$, the location of the zone boundary at time t may then be written[1]

$$l_s = \eta(t) c_m t \tag{6a}$$

where the function $\eta(t)$ depends on material and geometrical parameters and the form of $\varepsilon(t)$ and will be shown to be bounded by

$$0 < \eta(t) \le 1 \qquad . \tag{6b}$$

For the loading conditions considered, the additional boundary conditions at $z = l_s$ are:

$$\dot{u}_f = \dot{u}_m = \dot{u}_c \qquad (z = l_s) \tag{7a}$$

and

$$\varepsilon_f = \varepsilon_m = \varepsilon(t) \qquad (z = l_s). \tag{7b}$$

If the load history, $\varepsilon(t)$, possesses discontinuities, e.g., a step load, then discontinuities in stress and particle velocity will also propagate at the boundary of the process zone (e.g., Achenbach, 1973; see also Appendix A).

4. Composite Stress Rising Linearly in Time

A case of representative interest for dynamic bridged crack problems and for which analytical results can be found is that of a load or bridging traction that increases linearly in time. A linearly increasing load might give insight, for example, into bridging effects in a specimen in which substantial bending arises, such as a standard double cantilever

---

[1] It is easy to show that all the ensuing results for linearly rising loading, $\varepsilon = kt$, are unchanged if η is defined instead by writing $l_s = \eta(t) c_f t$; and thus do not depend on the relative magnitudes of c_f and c_m.

beam delamination specimen. In such specimens, the crack profile is often approximately linear and the rate of increase of the bridging tractions at any point might also be approximately linear if the crack propagates at approximately constant speed. The bridging traction at a particular material point might be expected to rise from zero as the delamination crack first passes until a peak value is reached, perhaps corresponding to bridging fibre rupture. Analytical results can be found for linearly increasing loads.

Let

$$\varepsilon(t) = kt \tag{8}$$

where k is constant and all displacements and boundary tractions are zero for $t < 0$. In this case, $\theta = 1$ and the wave equations have the solutions

$$u_f = -\frac{k}{c_m}\alpha z^2 + [1 + 2\eta\alpha]\varepsilon z \tag{9a}$$

$$u_m = \frac{k}{c_m}\frac{1}{2\eta}z^2 + \frac{1}{2}[1 + 2\eta\alpha]\varepsilon l_s \tag{9b}$$

where η is independent of time and satisfies

$$\alpha\eta^3 + \tfrac{1}{2}\eta^2 + \beta\alpha\eta - \tfrac{1}{2} = 0 \tag{9c}$$

with the dimensionless parameters α and β given by

$$\alpha = \frac{\tau c_m}{E_f R k} \qquad \& \qquad \beta = \frac{f}{1-f}\frac{E_f}{E_m} \tag{9d}$$

Analysis shows that Eq. (9c) has only one real root, which always lies in $(0,1)$.

The particle velocities and the strains for $0 \le z \le l_s$ are given by

$$\dot{u}_f = [1 + 2\eta\alpha]kz \tag{10a}$$

$$\dot{u}_m = [1 + 2\eta\alpha]kl_s \tag{10b}$$

$$\varepsilon_f = \left[1 + 2\eta\alpha\left(1 - \frac{z}{l_s}\right)\right]\varepsilon \tag{10c}$$

$$\varepsilon_m = \frac{z}{l_s}\varepsilon \tag{10d}$$

The matrix particle velocity is uniform and increases in proportion to l_s. The fibre velocity rises linearly through the process zone. A strain concentration, $\varepsilon_f/\varepsilon$, propagates in the fibre behind the process zone front, while the matrix strain in the process zone is always less than ε. The strain distributions and velocities beyond the process zone, $z > l_s$, need not be specified, provided the composite strain ε obeys the condition Eq. (7) on the process zone boundary.

The displacement, u, to be used in defining the traction law, $p(u)$, is given by the common fibre and matrix displacement, $u_1 = u_f(z = l_s) = u_m(z = l_s)$ at the boundary of the process zone minus the displacement expected if the process zone material were elastic:

$$u = u_1 - \varepsilon l_s$$

$$= \frac{c_m}{k}\alpha\eta^2\varepsilon^2$$

$$= \frac{c_m\alpha\eta^2}{kE^2}p^2 \qquad \qquad (11)$$

Equation (11) constitutes the traction law for the case of linearly rising loads.

The limit of very fast loading corresponds to $k \to \infty$, whereupon $\alpha \to 0$ and $\eta \to 1$, since the first and third terms in Eq. (9c) become negligible. The disturbance then propagates at the bar wave speed in the matrix.

Static loading is represented by the limit $k \to 0$ or $\alpha \to \infty$, for which the first two terms of Eq. (9c) become small and one has the asymptotic solution

$$\eta \to \frac{1}{2\alpha\beta} \qquad \qquad (12)$$

For this limit, substituting Eq. (12) into Eqs. (6a) and (11) yields

$$l_s \to \frac{1-f}{f}\frac{E_m R}{2\tau}\varepsilon \qquad \qquad (13a)$$

$$u \to u^{(st)} = \left(\frac{1-f}{f}\right)^2 \frac{E_m^2 R}{4E_f\tau}\varepsilon^2 \qquad \qquad (13b)$$

which coincide with the results obtained by McCartney (1987).[2]

Equations (10) and (13b) show that for loads that increase linearly with time, the form of the traction law is identical in the static and dynamic cases and

$$\frac{u}{u^{(st)}} = 2\alpha\beta\eta \qquad . \qquad (14)$$

Thus the strength of the effects arising from inertia is measured by the degree to which the limit of Eq. (12) is not approached. This can be conveniently summarised by comparing the product $2\alpha\beta\eta$ to unity.

Large β. Asymptotic analysis of Eq. (9c) shows that in the limit $\beta \to \infty$, $2\alpha\beta\eta \to 2\left[\sqrt{(\alpha\beta)^4 + (\alpha\beta)^2} - (\alpha\beta)^2\right]$ (second, third, and fourth terms of Eq. (9c) dominant), which is a function of $\alpha\beta$ and not of β separately; and Fig. 3a shows that this limit is approached quite closely for $\beta > 1$, which is expected, for example, for composites containing relatively stiff fibres ($E_f > E_m$). Fig. 3a also suggests that, as an engineering estimate, inertial effects are large when

$$\alpha\beta \equiv \frac{f}{1-f}\frac{\tau}{Rk}\frac{c_m}{E_m} \leq 2 \qquad (\beta > 1) \qquad . \qquad (15)$$

Remembering that k^{-1} is the time constant of the loading, this condition can be rewritten

$$k^{-1} < 2\frac{1-f}{f}\frac{E_m}{\tau}\frac{R}{c_m} \qquad (\beta > 1) \qquad . \qquad (16)$$

Small β. The limit of a relatively stiff matrix can be analysed by observing that $\alpha \propto E_m^{\frac{1}{2}}$ while $\beta \propto E_m^{-1}$; and that Eq. (9c) in the limit $E_m \to \infty$ therefore yields the limiting solution $\eta \to (2\alpha)^{-1/3}$ (first and last terms of Eq. (9c) dominant). Thus $2\alpha\beta\eta \to (2\alpha\beta)^{2/3}\beta^{1/3}$ when $\alpha\beta \to 0$. Figure 3b shows this approximation for three values of $\beta \leq 1$. While the limit is approached only for $\alpha\beta$ so small that $2\alpha\beta\eta$ is also small, it can nevertheless be used as the basis for engineering estimates of the condition for significant inertial effects, i.e., the first significant departure of $2\alpha\beta\eta$ from unity. The construction of Fig. 3b suggests that inertial effects will be significant when $\alpha\beta < 4(\alpha\beta)_1$, where $(\alpha\beta)_1$ is the value of the product $\alpha\beta$ at which the equation $(2\alpha\beta)^{2/3}\beta^{1/3} = 1$ is satisfied; i.e.,

---

[2] Marshall et al. (1985) derived expressions with different coefficients, but those of McCartney are to be preferred, since they correspond to a proper definition of the crack displacement and are consistent with conservation of energy.

$$\alpha\beta < \frac{2}{\beta^2} \qquad (\beta < 1). \qquad (17)$$

This leads to the criterion for significant inertial effects for composites with relatively stiff matrices that

$$k^{-1} < 2\left[\frac{1-f}{f}\right]^3 \frac{E_m^2}{E_f^2} \frac{E_m}{\tau} \frac{R}{c_m} \qquad (\beta < 1) \qquad . \qquad (18)$$

The criteria of Eqs. (16) and (18) coincide when $\beta = 1$.

Since $2\alpha\beta\eta < 1$ always, inertial effects increase the stiffness, dp/du, of the traction law for loads that increase linearly in time.

5. Fibre Pullout from a Rigid Matrix

Analytical results have not been obtained for other loading histories for the composite problem. (The matrix and fibre motions evolve in quite complicated ways for other cases.) However, results for the pullout of a single fibre from a rigid matrix to which it is coupled by friction can be found for step loads as well as linearly increasing loads. The problem considered for a rigid matrix is as shown in Fig. 4. The fibre is loaded on the fracture plane by tractions, $T(t)$, which can be represented by the boundary condition, $\varepsilon_0(t)$, for the axial strain in the fibre at $z = 0$. The response of the system that is of interest is wholly represented by the load point displacement, i.e., the displacement, $u_0(t)$, of the fibre at $z = 0$, since the matrix is rigid (motionless). Specifying a boundary condition on the fracture plane, rather than at the end of the slip zone, as for the composite problem, is preferred here because it allows a simpler statement of the step loading case.

Full solutions of this problem for step and linearly increasing loads are given in Appendix A. For the present discussion, the most interesting features are the following.

While the load point displacement is reduced by inertial effects for linearly increasing loads, for a step load it is increased. For a linearly increasing load, $\varepsilon_0 = kt$,

$$\frac{u_0}{u_0^{(st)}} = 2\left[\frac{\sqrt{1+(kt_r)^2}-1}{(kt_r)^2}\right] \qquad (19)$$

at any time, where the characteristic time of the system, t_r, is given by

$$t_r = \frac{E_f R}{\tau c_f} \qquad (20)$$

with the subscript "r" referring to the matrix being rigid. The ratio of Eq. (19) is plotted in Fig. 5. It is always less than unity. In contrast, for a step function load $\varepsilon_0(t) = \varepsilon_0$, a constant for $t > 0$, all motion ceases when $t = \varepsilon_0 t_r$, at which point $u_0 = 2u_0^{(st)}$: inertial effects double the displacement expected from loading statically to the same applied load. Correspondingly, the strain gradient left in the fibre following dynamic (step) loading is exactly half that found after static loading.

From these results, one can see that the following behaviour should be expected in the composite problem (with a compliant matrix) if a linearly increasing load is followed by a period of constant loading. If the composite strain has been increased linearly to some value ε at time t_1, the matrix and fibre will both be moving at the boundary of the process zone with (positive) velocities given by Eqs. (10a) and (10b) evaluated at $z = l_s$. To achieve this state, the still-intact composite itself must be accelerating towards positive z, maintaining the same velocity at $z = l_s$. If the composite strain is then fixed (no longer increasing), the composite will slow down and the matrix and fibre will begin to compress into the boundary of the process zone, under the influence of their inertia. This gives rise to quite complex motions, but the end result will be that the matrix will have displaced further relative to the fibre at the crack plane and the effective crack displacement, u, will have increased from its value at $t = t_1$. Analogy with the problem of the fibre being pulled out of a rigid matrix suggests that u might finally be larger than if the composite strain increased to the same level statically. However, this conjecture must be substantiated by numerical solutions.

6. Implications for Dynamic Bridged Cracks

Whether or not dynamic effects in the pullout process will be important in the problem of a propagating bridged crack will depend on the loading rate for the bridging element (stitch or rod). The loading rate will depend on the crack profile, which will depend on the specimen shape and the loading configuration. It will also depend on the crack propagation rate, but the onset of significant dynamic effects can be evaluated by considering the rate of change of displacements implied by static solutions to the instantaneous load.

The likely magnitude of inertial effects is analysed for two crack problems in the following. To derive analytical estimates based on the results obtained above, the composite strain at the boundary of the process zone must be assumed to rise linearly in time. Of course, this may not be the case – the dynamic crack propagation problem must be solved with a self-consistently derived dynamic traction law before the form of the rate of increase can be known. But assuming a linear increase will yield insight into the likely order of magnitude of inertial effects.

6.1 Steady-State, Fully-Bridged Crack – the ACK Limit

Consider first a crack that would propagate under static conditions to the so-called ACK limit, in which a uniform applied stress comes into equilibrium with the bridging stresses

provided by intact fibres in the far crack wake (Fig. 6). The ACK limit can be attained, for example, by a matrix crack in a ceramic matrix composite in an infinite specimen loaded in remote tension (Aveston, Cooper, and Kelly, 1971; Cox and Marshall, 1994). The static applied stress, σ_{ACK}, required to continue crack propagation in the ACK limit is invariant and the crack opening displacement in the far crack wake is uniform (Fig. 6). For a composite in which the bridging elements are coupled to the matrix by uniform friction, static analysis gives the following well-known results (e.g., McCartney, 1987; Appendix B in Massabò and Cox, 1999; Marshall and Cox, 1988). The critical stress, σ_{ACK}, is given by

$$\sigma_{ACK} = \left[\frac{3}{2}G_c\gamma\right]^{1/3} \tag{21}$$

where

$$\gamma = \frac{p}{\sqrt{u}} = \frac{2fE}{\left((1-f)E_m\right)}\left[\frac{E_f\tau}{R}\right]^{1/2} \tag{22}$$

and G_c is the critical crack tip energy release rate for the matrix crack. The bridging stress approaches close to σ_{ACK} at a characteristic distance, l_{ACK}, from the crack tip given by

$$l_{ACK} = \frac{\pi\overline{E}}{4}\left[\frac{3}{2}G_c\right]^{1/3}\gamma^{-4/3} \tag{23}$$

where $\overline{E}$ is an elastic constant that depends on the degree of anisotropy of the composite (defined, e.g., in Cox and Marshall, 1991). If the composite strain on the boundary of the process zone in the wake of the ACK crack is assumed to rise linearly in time, as in Eq. (8), then

$$k = \frac{\sigma_{ACK}/E}{l_{ACK}/c_d} \tag{24}$$

where c_d is the velocity of propagation of the delamination crack tip, which is assumed constant. Using Eq. (9d), the product $\alpha\beta$, which determines the magnitude of inertial effects for a linearly rising load, is then

$$\alpha\beta \approx \frac{\pi}{16}\frac{1-f}{f}\frac{\overline{E}}{E}\frac{E_m}{E_f}\frac{c_m}{c_d} \qquad \text{(ACK crack)} \qquad . \tag{25}$$

For the square root traction law, $p \propto u^{1/2}$, the friction stress, τ, the fibre radius, R, and the critical energy release rate for the matrix, G_c, do not appear in this expression, although they appear in l_{ACK} and σ_{ACK} separately (Eqs. (21) and (23)).

For composites satisfying $\beta > 1$, the criterion for significant inertial effects in the bridging mechanism is that $\alpha\beta < 2$ (Eq. (15)). For elastically homogeneous composites, $\overline{E} \approx E$ and $\alpha\beta$ depends only on f and the ratio of the wave speed c_m and the crack velocity c_d. For example, for $f = 0.5$, $\alpha\beta$ will have a value less than 2 if $c_d \geq (\pi/32)c_m$. The velocity of a crack propagating in the ACK configuration has not previously been calculated. However, if the crack is fully bridged, as in an unnotched composite exhibiting multiple matrix cracking, crack growth is known to be unstable (e.g., Cox and Marshall, 1994), so that crack velocities satisfying $c_d \geq (\pi/32)c_m$ would appear to be feasible.

For composites satisfying $\beta < 1$ ($\beta \sim 0.1$ would appear to be easily attainable), inertial effects will appear at crack velocities lower by a factor of β^2 (Eq. (18)).

Thus inertial effects are predicted to be significant for the ACK crack configuration for at least some common composites.

6.2 Wedge-Loaded Double Cantilever Beam

The double cantilever beam (DCB) specimen loaded dynamically by a flying wedge offers a relatively simple experimental approach to the mode I dynamic delamination problem (Fig. 7). The test is especially attractive for studying the bridging effects supplied by through-thickness reinforcement (e.g., stitches or rods) in laminates. An estimate of the likely role of inertia in bridging by stitches or rods follows. In the context of this paper, the "fibre" refers in this case to a stitch or rod and the "matrix" to the laminate.

For an increasing bridging traction law, i.e., a law for which $dp/du > 0$, the crack surfaces at the crack tip are predicted to come into contact in the DCB specimen under static loading at a certain crack length (Massabò and Cox, 2000). The crack will be arrested at this point, since the crack tip energy release rate must then vanish. Furthermore, the crack surfaces remain in contact when the applied load is increased so that the crack remains arrested and failure eventually ensues by another mechanism. An analogue of this interesting phenomenon of crack tip closure and crack arrest, which is a result of large scale bridging effects, might also be anticipated in dynamic loading (Beyerlein et al., 2000). An interesting case therefore is to consider the rate of opening of a crack that has arrested and is being loaded further by the flying wedge.

Simple analytical expressions for the opening displacements are available in the static case for a linear bridging law, $p = \beta_3 u$, and a composite with moderate levels of elastic anisotropy. If l is suitably large in Fig. 7, then the bending moment at the notch root, $x =$

0, will dominate over the shear load at $x = 0$. In this case, the crack will arrest after propagating a distance a_1 given by (Massabò and Cox, 2000)

$$a_1 = \frac{\pi}{2b} \tag{26}$$

where

$$b = \left[\frac{\beta_3}{4E_x' I_d} \right]^{\frac{1}{4}} \tag{27}$$

with $E_x' = E_x/(1 - \nu_{xy} \nu_{yx})$ (plane strain conditions assumed) and $I_d = 12/h^3$, with h the laminate half-thickness (see Fig. 7 for coordinates and dimensions). Insight into the magnitude of dynamic effects in the bridging phenomenon can be gained by considering the rate at which the crack opens at the end of the bridging zone ($x = 0$ in Fig. 7) under the influence of the wedge load when the crack length is fixed at $a = a_1$. From the results of Massabò and Cox (2000), the load point displacement, δ, at the point where the wedge contacts the specimen can be related for large l to the crack opening displacement, $\hat{u}_0$, at $x = 0$ (the last intact bridging element) by (see Appendix B)[3]

$$\delta = \frac{2}{\sqrt{3}} \left[\frac{\beta_3 l^4}{E_x' h^3} \right]^{\frac{1}{2}} \hat{u}_0 \tag{28}$$

The composite strain at the boundary of the process zone at $x = 0$ is

$$\varepsilon = \frac{\beta_3 \hat{u}_0}{E_3} \tag{29}$$

while, for a wedge subtending an angle 2ϕ and moving at velocity v_w,

$$\frac{d\delta}{dt} = v_w \tan\phi \tag{30}$$

If v_w is constant, Eqs. (28 – 30) yield a linear rate of increase for ε, where, in the notation of Eq. (8),

---

[3] These estimates are based on results for a linear bridging law. Equivalent results for a quadratic law, $p \propto u^{1/2}$, which is expected for static loading of fibers coupled to the matrix by friction, have not been published. However, the estimated times for reaching a given displacement and composite strain are likely to be of the same order of magnitude as for a linear law.

$$k = \frac{\sqrt{3}}{2}\left[\frac{E'_x \beta_3 h}{E_3^2}\right]^{1/2} \frac{hv_w \tan\phi}{l^2} \tag{31}$$

and thence

$$\alpha\beta = \frac{2}{\sqrt{3}} \frac{f}{1-f} \frac{\tau}{\sqrt{E'_x \beta_3 h}} \frac{E_3}{E_m} \frac{l^2}{hR} \frac{c_m}{v_w \tan\phi} \quad \text{(wedge-loaded DCB)} . \tag{32}$$

Here c_m refers to the bar wave speed in the laminate ("matrix") in the through-thickness direction. The modulus E_3 is that of the composite (with stitches or rods) in the through-thickness direction, while E_m is that of the laminate (without stitches or rods) in the same direction. If f is small, which is the usual case, $E_m \approx E_3$; and the factor $f/(1-f) \approx f$, with $f = 0.05$ a typical value. Experimental data for typical stitched laminates show $\beta_3 \approx 100$ MPa/mm (Massabò et al., 1998; Turrettini, 1996). Taking $E'_x = 60$ GPa and $h = 6$ mm, the factor $\sqrt{E'_x \beta_3 h}$ has the representative value 6 GPa. The ratio $\tau/\sqrt{E'_x \beta_3 h}$ will have typical values $\sim 10^{-3} - 10^{-2}$ ($\tau = 6 - 60$ MPa). With $l = 20$ mm, $R = 1$ mm, and $\phi = 20°$, for example, Eq. (32) reduces to the particular numerical estimate

$$0.01\frac{c_m}{v_w} \le \alpha\beta \le 0.1\frac{c_m}{v_w} \tag{33}$$

For composites for which $\beta > 1$ (including most stitched laminates), inertial effects will be significant (i.e., $\alpha\beta < 2$) provided $v_w > c_m/200$ ($\tau = 6$ MPa) or $v_w > c_m/20$ ($\tau = 60$ MPa).

Such wedge velocities are eminently attainable and inertial effects in the bridging law are likely to be significant in the wedge-loaded DCB test.

7. Discussion

The solutions presented here are based on the approximation that displacements are functions of z only. For static loading, this is an accurate approximation as long as the slip distance is large compared to the fibre diameter (Hutchinson and Jensen, 1990). The condition that the slip zone length should be much larger than the fibre diameter will be satisfied if the friction stress, τ, takes values typical in brittle matrix composites or polymer textile composites.

For dynamic problems, the conditions under which solutions that depend on z only will be accurate have not yet been studied. The solutions presented in this work will at least provide tentative limits against which three-dimensional numerical solutions can be compared.

Whether the approximation that displacements depend on z alone is accurate will also depend on the presence of a nonzero debond energy (energy required for separation of the fibres and the matrix). Here the debond energy was assumed to be zero (fibres and matrix already chemically separated). Dynamic analysis of materials in which the debond energy is not small will be significantly more complicated.

For stitched laminates, one of the cases assessed in Section 5, the requirement that the slip or process zone, l_s, be large compared to the fibre (stitch) diameter (typically 1 mm) implies that it will also be comparable to or greater than a typical laminate half-thickness, h ($\sim$ 6 mm). When the value of l_s predicted for an infinite body would exceed h, stress waves will reflect from the laminate surface, complicating the micromechanics of the process zone. These effects are not studied here.

A feature of the wave solutions for loads that increase monotonically from zero with time is that stress disturbances propagate away from the fracture plane at velocities other than either the matrix or fibre bar wave speed. This is the case for both the composite problem (Section 4) and the problem of a fibre being pulled out of a rigid matrix (Nikitin and Tyurekhodgaev, 1990; Appendix A). In the composite problem, the front velocity is always less than the matrix bar wave speed. The possibility exists that the front velocity will exceed the bar wave speed in the fibres, but numerical checks show that this can happen only for very high (and unlikely) ratios of fibre to matrix density.

No account has been attempted here of the conditions under which the strain at the boundary of the process zone, ε, can be expected to rise linearly in time, apart from the special case of a wedge loaded DCB specimen. The relationship between ε and the far field conditions in a dynamically loaded body will generally be complicated and revealed only by computational solutions of the dynamic stress propagation problem for the whole body, including the process zone. The particular problem of finding far field loading conditions that will result in $\varepsilon(t)$ being linear in time is very challenging.

8. Conclusions

Some analytical results have been presented for the problem of bridging by the mechanism of fibre pullout when the inertia of the fibre and the matrix are taken into account. Simple criteria have been specified for significant inertial effects in the bridging mechanism in representative mode I crack propagation problems. Inertial effects in the bridging mechanism will often be significant for a matrix crack propagating dynamically in the steady state ACK limit in a brittle matrix continuous fibre composite or delamination in laminates reinforced by through-thickness stitching or rods.

Significant inertial effects are favoured by low fibre volume fraction, low friction stress, low matrix bar wave speed, and low fibre modulus; and high fibre diameter and high matrix modulus. If the fibre modulus is high enough (relative to the matrix modulus), the criterion for inertial effects becomes independent of fibre modulus. The matrix density

enters the criterion only through the matrix bar wave speed. The criterion is always independent of the fibre density.

For pullout or bridging stresses that rise linearly in time, the instantaneous crack displacement is less in the presence of inertial effects than it would be under static loading to the same bridging stress. However, solutions for pullout from a rigid matrix suggest that, if the bridging stress rises rapidly and is then held at a constant value, the crack displacement when all particle motion finally stops will be greater than it would have been under static loading to that stress level. Thus regimes of both hardening and softening of the bridging traction law due to inertial effects can be expected in bridged crack problems.

Acknowledgments

References

J. D. Achenbach, *Wave Propagation in Elastic Solids*, North-Holland, 1973, pp. 138-143.

J. Aveston, G. A. Cooper, and A. Kelly, "Single and Multiple Fracture. The Properties of Fibre Composites," Conf. Proc., National Physical Lab., IPC Science and Tech. Press Ltd., pp. 15-24 (1971).

G. Bao and Z. Suo, "Remarks on Crack Bridging Concepts," *Applied Mech. Review*, 24, 355-366 (1992).

I. Beyerlein, N. Sridhar, and B. N. Cox, "Large Scale Bridging Effects in Dynamic Delamination," to be submitted to *J. Mech. Phys. Solids*.

B. N. Cox, "Extrinsic Factors in the Mechanics of Bridged Cracks," *Acta Metallurgica et Materialia* 39, 1189-1201 (1991).

B. N. Cox and D. B. Marshall, "Stable and Unstable Solutions for Bridged Cracks in Various Specimens," *Acta Metall. et Mater.* 39, 579-89 (1991).

B. N. Cox and D. B. Marshall, "Concepts for Bridged Cracks in Fracture and Fatigue," Overview No. 111, *Acta Metall. Mater.* 42, 341-63 (1994).

J. W. Hutchinson and H. M. Jensen, "Models of Fiber Debonding and Pullout in Brittle Composites with Friction," *Mechanics of Materials*, 9, 139-163 (1990).

L. K. Jain and Y.-W. Mai, "Determination of Mode II Delamination Toughness of Stitched Laminated Composites," *Composites Sci. and Tech.*, 55, 241-253 (1995).

L. N. McCartney, "Mechanics of Matrix Cracking in Brittle-Matrix Fibre-Reinforced Composites," *Proc. Roy. Lond.* A409, 329-350 (1987).

D. B. Marshall and B. N. Cox, "A J-Integral Method for Calculating Steady-State Matrix Cracking in Composites," *Mechanics of Materials* 7, 127-33 (1988).

D. B. Marshall, B. N. Cox and A. G. Evans, "The Mechanics of Matrix Cracking in Brittle-Matrix Fiber Composites," *Acta Metall.* 33, 2013-2021 (1985).

R. Massabò and B. N. Cox, "Concepts for Bridged Mode II Delamination Cracks," *J. Mech. Phys. Solids*, 47, 1265-1300 (1999).

R. Massabò and B. N. Cox, "Unusual Characteristics of Mixed Mode Delamination Fracture in the Presence of Large Scale Bridging," *Mechanics of Comp. Mater. and Struct.*, in press.

L. V. Nikitin and A. N. Tyurekhodgaev, 1990, "Wave Propagation and Vibration of Elastic Rods with Interfacial Frictional Slip," *Wave Motion*, **12**, 513-526.

A. Turrettini, Masters Thesis, University of California, Santa Barbara, 1996.

Appendix A. Fibre Pullout from a Rigid Matrix.

Solutions are exhibited here to the problem described in Fig. 4 and related text.[4] Since the matrix is rigid, it experiences no motion. The motion of the fibre is governed by the wave equation of Eq. (2a). The problem is defined by stating the value of the load applied to the end of the fibre at $z = 0$, rather than the matrix strain at the end of the process zone.

Boundary Conditions for Front of Propagating Disturbance

Let the location of the front limiting the extent of the stress disturbance caused by waves propagating along the fibre be written $l_r = \eta c_f t$, where the applied load is turned on at time $t = 0$. (The subscript "r" is used for this problem as a mnemonic for "rigid" matrix.) The jump in the stress, $\Delta\sigma_f$, and jump in particle velocity, $\Delta\dot{u}_f$ (where $\dot{u}_f \equiv \partial u_f/\partial t$), across the front, i.e., from $z > \eta c_f t$ to $z < \eta c_f t$, must satisfy the energy-conserving relation expected from integration of the impulse across the front, namely (see, e.g., Achenbach, 1973)

$$\Delta\dot{u}_f = -\frac{\Delta\sigma_f}{\rho_f v_0} \tag{A.1}$$

where v_0 is the velocity of the front, $v_0 = c_f \partial(\eta t)/\partial t$. To ensure integrity of the fibre, the displacement must be continuous across the front, i.e.,

$$u_f(z,t) = 0 \qquad\qquad (z \rightarrow l_r^-) \qquad . \tag{A.2}$$

Two front conditions may now be distinguished. If a stress discontinuity exists at the front, $\Delta\sigma_f > 0$, then kinematic considerations along with Eq. (A.1) necessitate that (see, e.g., Achenbach, 1973)

$$\eta = 1 \qquad\qquad (\Delta\sigma_f > 0) \tag{A.3a}$$

or, equivalently, $v_0 = c_f$. If the stress is continuous across the front, i.e., $\sigma_f = 0$ at $z = z_f$, then the velocity of the front remains indeterminate:

$$0 < \eta < 1 \qquad\qquad (\Delta\sigma_f = 0) \qquad . \tag{A.3b}$$

---

[4] The same problem of an end-loaded rod damped by friction was also solved for various cases by Nikitin and colleagues in the 1960's. These slightly arcane Russian publications are summarised in Nikitin and Tyurekhodgaev (1990), which itself has been cited only once previously in the western literature. In the following, dynamic solutions are developed for the cases of particular interest to the delamination problem, with emphasis on the relationship between the dynamic results and the static limit. Some minor errors in Nikitin and Tyurekhodgaev for the case of loading that is linear in time are corrected.

Solutions obeying both Eqs. (A.3a) and (A.3b) will be demonstrated in the following.

Step function Load

Consider first a step function load such that

$$E_f \frac{\partial u_f}{\partial z}\bigg|_{z=0} = E_f \varepsilon_0 \qquad \text{for } t > 0 \qquad . \tag{A.4}$$

Since a stress discontinuity is implied by a propagating step load, the front conditions given by Eqs. (A.1), (A.2), and (A.3a) are expected to apply. The solution to the wave equation, Eq. (2a), that satisfies these boundary conditions is

$$u_f = -\frac{\tau}{2RE_f}\left(z^2 - c_f^2 t^2\right) + \varepsilon_0\left(z - c_f t\right) \tag{A.5}$$

with $\eta = 1$ (front velocity $v_0 = c_f$) always. The particle velocity is thus

$$\frac{\partial u_f}{\partial t} = \frac{\tau}{RE_f}c_f^2 t - \varepsilon_0 c_f = c_f \frac{t}{t_r} \tag{A.6a}$$

where

$$t_r = \frac{E_f R}{\tau c_f} \tag{A.6b}$$

and is independent of z: within the sliding zone $0 < z < c_f t$, the fibre moves with uniform velocity. The particle acceleration is given by

$$\frac{\partial^2 u_f}{\partial t^2} = \frac{\tau}{RE_f}c_f^2 = \frac{c_f}{t_r} \tag{A.7}$$

which is uniform in time. Motion stops when

$$t = \varepsilon_0 t_r \qquad . \tag{A.8}$$

This is the characteristic time of the dynamic process for the case of a rigid matrix. At $t = \varepsilon_0 t_r$, the sliding zone has advanced a distance

$$l_r = c_f t_r \varepsilon_0 = \frac{E_f R}{\tau}\varepsilon_0 \qquad (t = \varepsilon_0 t_r) \tag{A.9}$$

The strain along the rod has the distribution

$$\frac{\partial u_f}{\partial z} = \varepsilon_0 - \frac{\tau}{RE_f}z \qquad . \tag{A.10}$$

The load point displacement, u_0, (i.e., the displacement at $z = 0$) evolves in time according to

$$u_0 = -\varepsilon_0 c_f t \left[1 - \frac{1}{2\varepsilon_0}\frac{t}{t_r} \right] \qquad . \tag{A.11}$$

When $t = \varepsilon_0 t_r$,

$$u_0 = -\frac{E_f R}{2\tau}\varepsilon_0^2 \qquad (t = \varepsilon_0 t_r) \tag{A.12}$$

which is exactly twice the displacement, $u_0^{(st)}$, developed under static loading (see below). The final slip length, l_r, is also twice the slip length for static loading; and the strain gradient, $\partial u_f / \partial z$, is half that developed under static loading.

One important consequence of the last fact is that when motion is arrested at $t = \varepsilon_0 t_r$, no further stress relaxation is required: the stress gradient at $t = \varepsilon_0 t_r$ is only half the maximum gradient that can be supported in the fibre by the friction tractions. According to the constitutive behaviour assumed for the friction phenomenon, Eq. (1c), the fibre will remain motionless. Therefore, the configuration predicted for $t = \varepsilon_0 t_r$ is the final configuration. Since Eq. (A.10) predicts that $\sigma_f(l_r) = 0$ at $t = \varepsilon_0 t_r$, the front condition will switch at this instant to Eq. (A.3b): the condition of Eq. (A.1) leads to an indeterminate front velocity.

When the fibre arrests at $t = \varepsilon_0 t_r$, the particle acceleration in the slip zone falls instantaneously to zero from the constant value of Eq. (A.7). At the same instant, the friction tractions along the slip zone fall from the uniform value, τ, which they had during the motion of the fibre, to $\tau/2$, the value required to sustain the stress gradient in the fibre at the time of arrest. This discontinuous change in the friction stress is a direct consequence of the constitutive behavior embodied in Eq. (1).

For the step load case, Eq. (A.5) yields the following energy analysis. The work done by the load at time $t < \varepsilon_0 t_r$ is given by

$$W_1 = \pi R^2 E_f \varepsilon_0 u_0 = \frac{\pi E_f^2 \varepsilon_0^3 R^3}{\tau}\left(\frac{t}{\varepsilon_0 t_r} \right)\left[1 - \frac{1}{2}\left(\frac{t}{\varepsilon_0 t_r} \right) \right] \qquad . \tag{A.13}$$

The kinetic energy in the moving fibre at time t is given by

$$W_k = \int_0^{c_f t} \frac{\pi R^2 \rho_f}{2} \left(\frac{\partial u_f}{\partial t}\right)^2 dz = \frac{\pi E_f^2 \varepsilon_0^3 R^3}{2\tau} \left(\frac{t}{\varepsilon_0 t_r}\right)\left[\left(\frac{t}{\varepsilon_0 t_r}\right)-1\right]^2 . \tag{A.14}$$

The strain energy in the fibre at time t is given by

$$W_e = \int_0^{c_f t} \frac{\pi R^2 E_f}{2} \left(\frac{\partial u_f}{\partial z}\right)^2 dz = \frac{\pi E_f^2 \varepsilon_0^3 R^3}{2\tau} \left(\frac{t}{\varepsilon_0 t_r}\right)\left[1-\left(\frac{t}{\varepsilon_0 t_r}\right)+\frac{1}{3}\left(\frac{t}{\varepsilon_0 t_r}\right)^2\right] . \tag{A.15}$$

These energy dissipated in friction up to time t is given by

$$W_f = -\int_0^{c_f t} 2\pi R \tau u dz = \frac{\pi E_f^2 \varepsilon_0^3 R^3}{\tau} \left(\frac{t}{\varepsilon_0 t_r}\right)^2\left[1-\frac{2}{3}\left(\frac{t}{\varepsilon_0 t_r}\right)\right] . \tag{A.16}$$

The energy terms are plotted in Fig. A.1. The total work done at time $t = \varepsilon_0 t_r$ is exactly three times that done in static loading to $\varepsilon_0 E_f$ (see below).

Linearly Increasing Load

Consider next the case of an applied strain that is given by the linear law

$$\sigma_f(0) = E_f \left.\frac{\partial u_f}{\partial z}\right|_{z=0} = E_f k t \qquad (t>0) . \tag{A.17}$$

In this case, a physically meaningful solution is found only for the front condition given by $\Delta\sigma_f = 0$ and Eq. (A.3b). With these boundary conditions, Eq. (2a) has the solution

$$u_f(z,t) = -\frac{\tau z^2}{2RE_f}\left[\sqrt{1+(kt_r)^2}+1\right] - \frac{\tau c_f^2 t^2}{2RE_f}\left[\sqrt{1+(kt_r)^2}-1\right] + ktz$$

$$= -\frac{\tau}{RE_f}\frac{1}{1-\eta^2}(z-\eta c_f t)^2$$

$$(z \leq \eta c_f t) \tag{A.18}$$

with

$$\eta = kt_r \Big/ \left[\sqrt{1+(kt_r)^2}+1\right] \tag{A.19}$$

where t_r is the characteristic time of Eq. (A.8). Thus the particle velocity is given by

63

$$\frac{\partial u_f}{\partial t} = -\frac{\tau c_f^2 t}{RE_f}\left[\sqrt{1+(kt_r)^2}-1\right]+kz \qquad (z \le \eta c_f t) \qquad \text{(A.20)}$$

the acceleration by

$$\frac{\partial^2 u_f}{\partial t^2} = -\frac{\tau c_f^2}{RE_f}\left[\sqrt{1+(kt_r)^2}-1\right] \qquad (z \le \eta c_f t) \qquad \text{(A.21)}$$

the stress distribution by

$$\sigma_f = kE_f t - \frac{\tau z}{R}\left[\sqrt{1+(kt_r)^2}+1\right] \qquad (z \le \eta c_f t) \qquad \text{(A.22)}$$

and the load point displacement by

$$u_0 = -\frac{\tau c_f^2 t^2}{2RE_f}\left[\sqrt{1+(kt_r)^2}-1\right] \qquad (t > 0) \qquad . \qquad \text{(A.23)}$$

The static limit in this case can be found by taking the limit $k \to 0$. One finds

$$\eta c_f t \to \frac{E_f R k t}{2\tau} = \frac{\sigma_f(0,t)R}{2\tau} = l_r^{(st)} \qquad (k \to 0) \qquad \text{(A.24a)}$$

$$\frac{\partial u_f}{\partial t} \to k\left[z - \frac{\sigma_f(0,t)}{\tau}R\right] \to 0 \qquad (k \to 0) \qquad \text{(A.24b)}$$

$$\sigma_f \to \sigma_f(0,t)\left[1 - \frac{2\tau}{\sigma_f(0,t)}\frac{z}{R}\right] = \sigma_f^{(st)} \qquad (k \to 0) \qquad \text{(A.24c)}$$

$$u_0 \to \frac{E_f R}{4\tau}(kt)^2 = \frac{[\sigma_z(0,t)]^2 R}{4E_f\tau} = u_0^{(st)} \qquad (k \to 0) \qquad \text{(A.24d)}$$

where the superscript "(st)" indicates the result obtained by static analysis for loading to the instantaneous value, $\sigma_z(0,t)$, of the applied tractions (see below). In the static limit, Eq. (A.24b) also shows that $\eta \to 0$ (consistently with Eq. (A.24a)); while in the limit of very rapid loading ($k \to \infty$), or vanishing friction ($\tau \to 0$), Eq. (A.24b) leads to $\eta \to 1$, i.e., the front reverts to propagating at the bar wave velocity.

Equations (A.23) and (A.24d) allow the dynamic load point displacement to be related very simply to the displacement expected for static loading to the same instantaneous applied load:

$$\frac{u_0}{u_0^{(st)}} = 2\left[\frac{\sqrt{1+(kt_r)^2}-1}{(kt_r)^2}\right] \qquad . \qquad (A.25)$$

The same characteristic time, t_r, identifies cases where dynamic effects are important in both the step and linear loading cases.

The Static Problem

Under static loading to stress $\sigma_0 = E_f \varepsilon_0$, force equilibrium leads to a linear stress gradient along the fibre

$$\sigma_f^{(st)} = \sigma_0\left[1-\frac{2\tau z}{\sigma_0 R}\right] \qquad (A.26)$$

so that the slip length, where $\sigma_f^{(st)} = 0$, is given by

$$l_r^{(st)} = \frac{E_f R}{2\tau}\varepsilon_0 \qquad . \qquad (A.27)$$

The load point displacement can be found by integrating the strain along the fibre and is given by

$$u_0^{(st)} = -\frac{E_f R}{4\tau}\varepsilon_0^2 \qquad . \qquad (A.28)$$

The total work done by the load in the static problem is given by

$$W_1^{(st)} = \int_0^{u_0^{(st)}} \pi R^2 \sigma du = \frac{\pi E_f^2 \varepsilon_0^3 R^3}{6\tau} \qquad (A.29)$$

where here u and σ denote the displacement and stress at $z = 0$ during loading.

Appendix B. The Wedge-Loaded DCB Specimen with Large Scale Bridging.

In a specimen in which shear deformation may be neglected (material anisotropy not too large) and in which a linear bridging law, $p = \beta_3 u$, acts on the bridged part of the crack (Fig. 7), analytical expressions can be found for the characteristics of crack propagation (Massabò and Cox, 2000). The crack displacement profile is given by

$$u = e^{bx}\left(c_1 \cos bx + c_2 \sin bx\right) + e^{-bx}\left(c_3 \cos bx + c_4 \sin bx\right) \tag{B.1}$$

where

$$b = \left[\frac{\beta_3}{4E_x' I_d}\right]^{1/4} \tag{B.2}$$

and $I_d = h^3/12$, $E_x' = E_x/(1 - \nu_{yx}\nu_{xy})$, and E_x and ν_{yx} and ν_{xy} are Young's modulus and Poisson's ratios for the laminate, respectively. The constants c_i are determined by boundary conditions. At the crack tip, $u = 0$ and the bending rotation $\phi = - du/dx = 0$ (shear deformation neglected); while at the notch root, $x = 0$, one can write generally that $u = \hat{u}_0$ and $\phi = \hat{\phi}_0$. Observing that the bending moment, $\hat{M} = M(x = 0)$, and shear force, $\hat{Q} = Q(x = 0)$, at $x = 0$ are related by

$$\frac{\hat{M}}{\hat{Q}} = -\frac{Pl}{P} = -l \tag{B.3}$$

where P is the load applied by the wedge and, for a beam with negligible shear deformation, $Q = -(E_x' I_d)d^3u/dx^3$ and $M = -(E_x' I_d)d^2u/dx^2$, one finds by solving for the coefficients c_I in (B.1) that

$$\hat{\phi}_0 = \frac{-b\hat{u}_0\left[e^{-\pi} + 1 + 2lb\left(e^{-\pi} - 1\right)\right]}{e^{-\pi} - 1 + lb\left(e^{-\pi} + 1\right)} \tag{B.4}$$

and thence

$$\hat{M} = -2\hat{u}_0 \frac{lb^3 E_x' I_d\left(e^{-\pi} + 1\right)}{e^{-\pi} - 1 + lb\left(e^{-\pi} + 1\right)} \tag{B.5}$$

If the loading arm length, l, is not short, then the deflection at the point of contact with the flying wedge, δ, will be much greater than u_0 and therefore δ can be estimated as the deflection expected for a cantilever beam with built-in end condition at $x = 0$:

$$\delta = -\frac{\hat{M}l^2}{3E_x'I_d} \tag{B.6}$$

and thus

$$\delta = \frac{2}{3}\hat{u}_0 l^2 b^2 \frac{e^{-\pi}+1}{e^{-\pi}+1+(lb)^{-1}(e^{-\pi}-1)} \tag{B.7}$$

In the limit that lb is large,

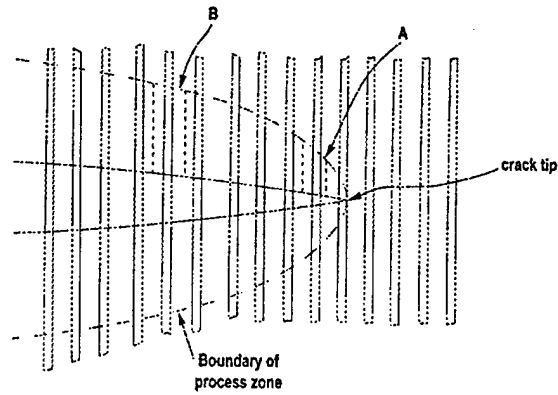$$\delta \approx \frac{2}{\sqrt{3}}\left[\frac{\beta_3 l^4}{E_x' h^3}\right]^{\frac{1}{2}}\hat{u}_0 \tag{B.8}$$

Figure Captions

1. (a) Schematic of a crack bridged by fibres, showing process zone where relative displacement exists between fibres and matrix. (b) Idealisation of the bridged crack problem with process zone replaced by surface tractions acting on the fracture surfaces.

2. Schematic of the dynamic pullout problem in a representative volume near the fracture plane.

3. The product $2\alpha\beta\eta$, which indicates the relative importance of inertial effects in the bridging phenomenon. (a) Numerical results for representative values of β. (b) Numerical results for $2\alpha\beta\eta$ compared with asymptotic limit for large E_m (dashed curves). The value of $(\alpha\beta)_1$ is marked for $\beta = 0.01$ and is to be compared with the value of $\alpha\beta$ at which $2\alpha\beta\eta \approx 0.9$, which is taken as a representative cutoff for significant inertial effects.

4. Fibre pullout from a rigid matrix.

5. The ratio of dynamic and static load point displacements for a fibre pulled out of a rigid matrix by a load that rises linearly with time.

6. A matrix crack propagating in the ACK limit.

7. A double cantilever beam specimen loaded by a flying wedge.

A.1 The distribution of energy as a function of time for a fibre pulled out of a rigid matrix by a step load.

(a)

(b)

Figure 1

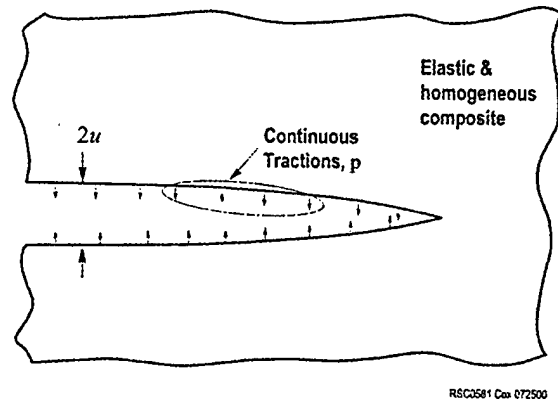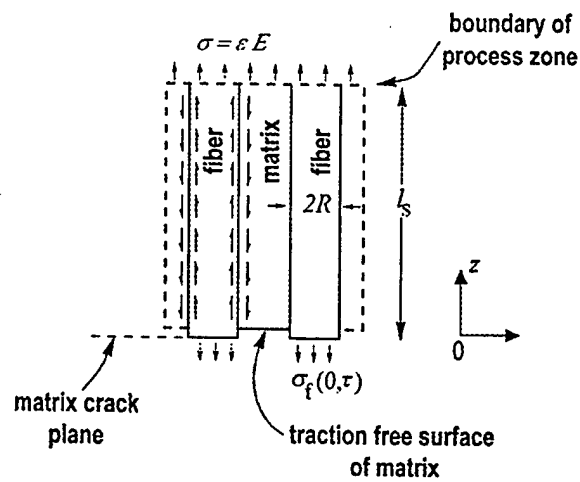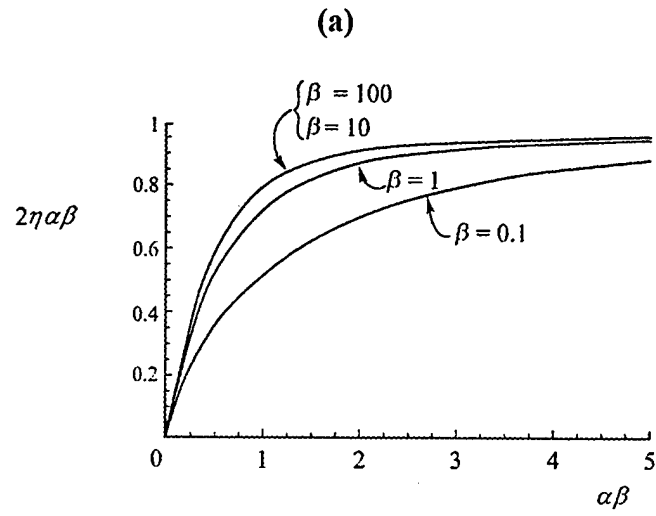

Figure 2

(a)

RSC0563 Cox 060500

(b)
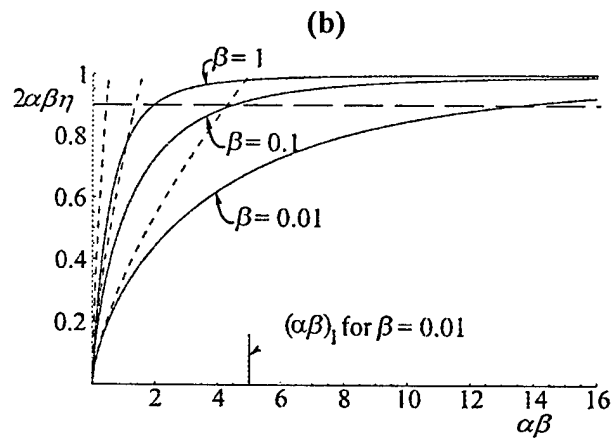
RSC0600.COX.0607.00

Figure 3
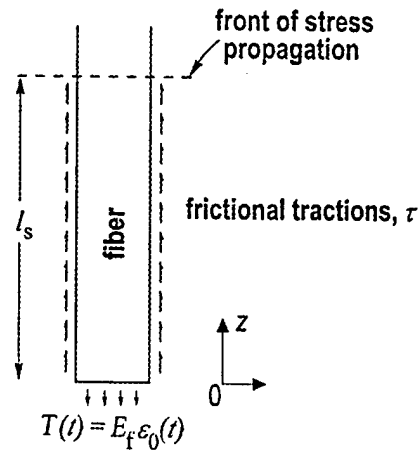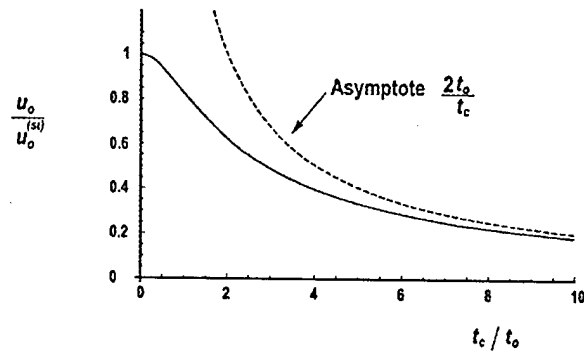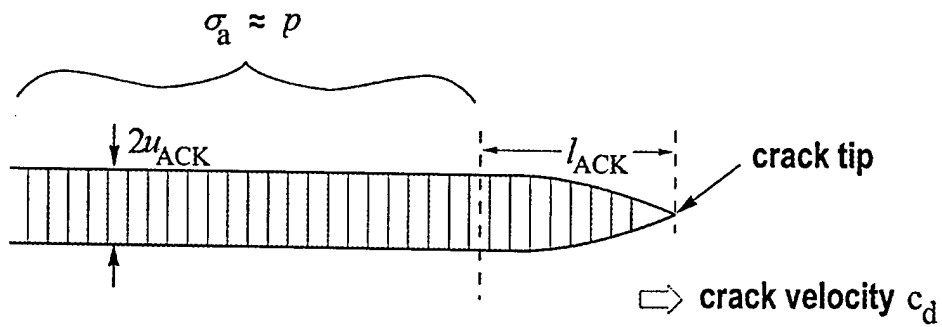
Figure 4.

Figure 5.

Figure 6.

RSC0571 Cox 072500

Figure 7.

$$\text{energy} \Big/ \left[\frac{\pi \sigma_o R^3}{\tau E} \right]$$

time, t/t_c
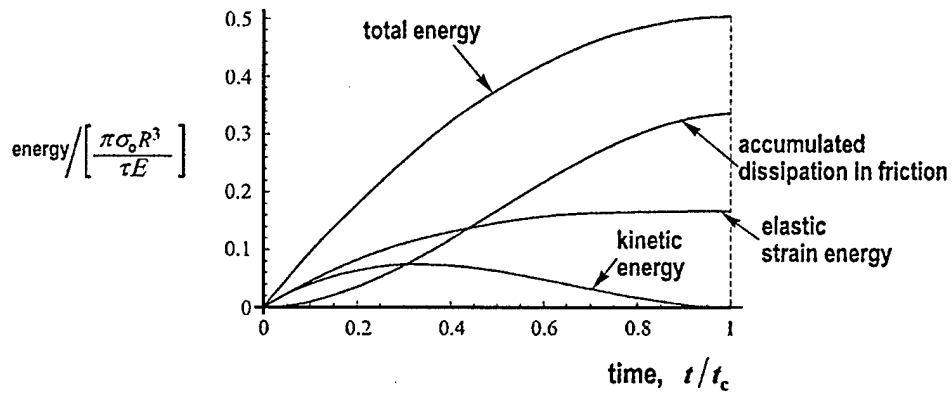
RSC0574 Cox 080500

Figure A.1

Simple form for the Dynamic $G - K$ relationship in Orthotropic Materials

N. Sridhar and B. N. Cox
Rockwell Science Center
1049 Camino Dos Rios
Thousand Oaks, CA 91360
U.S.A.

and

I. J. Beyerlein
Los Alamos National Laboratory
Los Alamos, New Mexico
U.S.A.

1. Introduction

This note presents explicit relations between the dynamic crack energy release rate and crack tip stress intensity factors in a form most amenable to computational work for a crack propagating along any principal axis in an orthotropic material. The results presented in this form may be particularly useful for work on delamination cracks in laminated composites, which are orthotropic in many important applications.

Prior work in the literature that treats the problem of interest here include the analysis of a mode I crack in an orthotropic medium by Piva and Viola (1988); and the analysis of a mixed mode crack in a transversely isotropic medium by Wu (1989). Yang and co-workers (1991) presented results for a mixed mode crack in an orthotropic material, but in a form that is not best suited for immediate computation. By an adaptation of the Stroh method of analysis used by Wu, the results of Yang et al. are rendered here in a different form better suited to numerical evaluation. The role of orthotropic anisotropy in determining the velocity dependence of G_d is then illustrated for delamination cracks in typical ceramic, metal and polymer matrix laminated composites.

2. Results

The relation between the energy release rate and the crack tip stress intensity factor is central to fracture analysis. It appears, for example, in the derivation of stress intensity factors from applications of the J-integral and in the derivation via energy arguments of integral equations for bridged cracks from weight functions. Details of the latter for dynamic cracks with large scale bridging in the crack wake will appear elsewhere.

Freund (1972) showed that the dynamic crack energy release rate for an extending crack in an elastic body can be written as the modified J-integral, which leads to the G-k relationship in the following, convenient form:

$$G_d = \frac{1}{2} k^D(t)^T L^{-1} k(t) \tag{1}$$

where G_d is the dynamic crack energy release rate and $k(t)$ is the instantaneous crack tip stress intensity factors (see Eq. 4.19 in Wu and references therein). The elements of the L^{-1} matrix are universal functions, in the sense that they are independent of the details of the applied loading or on the configuration of the body being analyzed. We present results for the L^{-1} matrix when the material possesses orthotropic symmetry and when the crack is extending along one of the principal axis. In this case, the off-diagonal elements of the matrix are zero and the diagonal elements of the L^{-1} matrix is just dependent on the elastic properties of the orthotropic medium and the instantaneous value of the crack tip velocity. For an orthotropic material with the crack propagating along the 1 direction (and direction 3 being the plane strain direction), elements of the L^{-1} matrix are:

$$L^{-1} = \frac{1}{C_{66}} \begin{pmatrix} \dfrac{-(\gamma_5 + \gamma_1\gamma_4)}{(\gamma_4^2 - \gamma_3\gamma_5)} & 0 & 0 \\ 0 & \dfrac{-(\gamma_3 - \gamma_2\gamma_4)}{(\gamma_4^2 - \gamma_3\gamma_5)} & 0 \\ 0 & 0 & \dfrac{1}{\gamma_6} \end{pmatrix} \tag{2}$$

where the γ's are

$$\gamma_1 = \frac{C_{66} - \beta_2^2 C_{22} - \rho v^2}{\beta_2(C_{12} + C_{66})} \qquad \gamma_2 = \frac{C_{11} - \beta_1^2 C_{66} - \rho v^2}{\beta_1(C_{12} + C_{66})} \qquad \gamma_3 = \frac{C_{11} + \beta_1^2 C_{12} - \rho v^2}{\beta_1(C_{12} + C_{66})}$$

$$\gamma_4 = \frac{C_{12} + \beta_2^2 C_{22} + \rho v^2}{(C_{12} + C_{66})} \qquad \gamma_5 = \frac{C_{12} + \beta_2^2 C_{22} - \dfrac{C_{12}}{C_{66}}\rho v^2}{\beta_2(C_{12} + C_{66})} \qquad \gamma_6 = \frac{C_{44}}{C_{66}}\beta_3$$

$$\tag{3}$$

where C_{ij} are coefficients of the stiffness matrix, ρ is the density of the medium and v is the instantaneous velocity of the crack tip. The expressions for β are:

$$\beta_1 = \sqrt{\frac{r_1 + \sqrt{r_1^2 - r_2}}{2\, C_{22}\, C_{66}}} \qquad \beta_2 = \sqrt{\frac{r_1 - \sqrt{r_1^2 - r_2}}{2\, C_{22}\, C_{66}}} \qquad \beta_3 = \sqrt{\frac{C_{55} - \rho v^2}{C_{44}}}$$

$$(4)$$

where

$$r_1 = C_{11} C_{22} - C_{12}^2 - 2 C_{12} C_{66} - (C_{22} + C_{66}) \rho v^2$$

and

$$r_2 = 4 C_{22} C_{66} (C_{11} - \rho v^2)(C_{66} - \rho v^2) \quad .$$

The $L^{-1}{}_{3,3}$ matrix elemenet is

$$L^{-1}{}_{3,3} = \frac{1}{C_{44} \sqrt{\dfrac{C_{55}}{C_{44}} - \dfrac{\rho v^2}{C_{44}}}}$$

$$(5)$$

We can also define the generalized Rayleigh wave function R(v) as

$$R(v) = \gamma_4^2 - \gamma_3 \gamma_5$$

$$(6)$$

and the Rayleigh wave speed (v_r) is obtained by setting $R(v_r) = 0$.

In the next section, the diagonal elements $L^{-1}{}_{1,1}$ and $L^{-1}{}_{2,2}$ are plotted numerically for cracks propagating along different principal axes in various representative composites. The L^{-1} matrix elements are functions of the elastic properties and the instantaneous crack velocity. Each diagonal element approaches the corresponding static value as $v \rightarrow 0$ and has the property of $O[(v_r - v)^{-1}]$ as $v \rightarrow v_r$, where v_r is the Rayleigh wave speed.

3. Discussion

In this section, we will present results for the the mode I and mode II contributions to the crack energy release rate, as represented by the $L^{-1}{}_{1,1}$ and $L^{-1}{}_{2,2}$ matrix elements, for various representative composites that possess orthotropic symmetry and where the crack

76

is extending along one of the principal axis. These results are presented graphically as a function of the orthotropy parameters and the instantaneous crack tip velocity. The mode III contribution to the crack energy release rate is a simple expression (see Eq. 5) and hence will not be examined further.

In the results presented below, the orientation is such that the principal axes of orthotropic symmetry are aligned with the coordinate axis, the crack lies in the 1-3 plane and the crack is propagating along the 1 direction (with direction 3 being the plane strain direction). Table I shows the stiffness tensor for various representative composites, the corresponding orthotropy paramaters and the Rayleigh velocity (v_r) normalized by the shear wave velocity (v_s). Also examined in Table I are cases where the crack is running along the different principal directions of orthotropic symmetry. The orthotropy parameters λ and ρ as presented by Suo, et al. (1991) are:

$$\lambda = \frac{b_{11}}{b_{22}} \quad \text{and} \quad \rho = \frac{b_{12} + \frac{1}{2}b_{66}}{\sqrt{b_{11}b_{66}}} \quad \text{where}$$

$$b_{ij} = \begin{cases} S_{ij} \ (plane \ stress) \\ S_{ij} - \dfrac{S_{i3}S_{j3}}{S_{33}} \ (plane \ strain) \end{cases}$$

and where S_{ij} are the elements of the compliance tensor.

Figure 1 shows the variation of the normalized $L^{-1}_{1,1} / [L^{-1}_{1,1}]_{static}$, where $[L^{-1}_{1,1}]_{static}$ is the value of $L^{-1}_{1,1}$ when $v \to 0$, as a function of the normalized crack velocity v/v_r, where v_r is the Rayleigh wave speed. This variation is shown for the different cases listed in Table I. However, it is clear from the figure that the variation in the crack energy release rate can be rationalized in terms of the orthotropy parameters λ and ρ. For the same normalized crack speed, the normalized mode I contribution ($L^{-1}_{1,1} / [L^{-1}_{1,1}]_{static}$) to the dynamic crack energy release rate increases as λ monotonically increases and as ρ monotonically decreases.

Figure 2 similarly shows the variation of the normalized $L^{-1}_{2,2} / [L^{-1}_{2,2}]_{static}$, where $[L^{-1}_{2,2}]_{static}$ is the value of $L^{-1}_{2,2}$ when $v \to 0$, as a function of the normalized crack velocity v/v_r, where v_r is the Rayleigh wave speed. This variation is shown for the different cases

listed in Table I. As in the mode I case, the variation in the crack energy release rate can be rationalized in terms of the orthotropy parameters λ and ρ. For the same normalized crack speed, the normalized mode II contribution ($L^{-1}_{2,2} / [L^{-1}_{2,2}]_{static}$) to the dynamic crack energy release rate increases as λ increases and as ρ decreases. However, as opposed to the mode I case, the variation on λ and ρ is much smaller. In addition, we observe that although the energy release rate shows a monotonic dependence on λ, the dependence on ρ, for small ρ, is not monotonic.

4. Conclusions

An analytical form for easy estimation of the dynamic crack energy release rate, in terms of the crack tip stress intensity factors, has been presented for cracks propagating along any of the principal axis in orthotropic material systems. The dynamic crack energy release rate depends on the magnitude of the two orthotropic parameters and the instantaneous crack tip velocity. The dynamic crack energy release rate is $O[(v_r - v)^{-1}]$ as $v \rightarrow v_r$, and where v_r is the Rayleigh wave speed. The variation in the dynamic crack energy relase rate for orthotropic materials can be rationalized in terms of the two orthotropy parameters λ and ρ.

References

Piva, A., and Viola, E., 1988, "Crack Propagation in an Orthotropic Medium", *Engineering Fracture Mechanics*, vol.29, 535-548

Freund, L.B., 1972, "Energy flux into the tip of an extending crack in an elastic solid", *Journal of Elasticity*, vol. 2, 341-349

Wu, K.-C., 1989, "On the crack tip fields of a dynamically propagating crack in an anisotropic solid", *Intl. Journal of Fracture*, vol. 41, 253-266

Yang, W., Suo, Z., and Shih, C.F., 1991, "Mechanics of dynamic debonding", *Proc. R. Soc. Lond. A*, vol. 433, 679-697

Suo, Z., Bao, G., Fan, B., and Wang,T.C., 1991, "Orthotropy Rescaling and Implications for Fracture in Composites", *Int. J. Solids. Structures*, vol.28, 235-248

Figure Caption

Figure 1: The variation of $L^{-1}_{1,1}$ (Fig.1a) and $L^{-1}_{2,2}$ (Fig.1b) normalized by their corresponding static values as a function of the crack tip velocity, normalized by the Rayleigh wave velocity, is shown for different values of λ and ρ.

Table I

|		C11 GPa	C22 GPa	C33 GPa	C44 GPa	C55 GPa	C66 GPa	C12 GPa	C13 GPa	C23 GPa	λ	ρ	v_r/v_s
Carbon/Epoxy Unidirectional composite	1a	150	12	12	5	30	30	5	5	5	0.08	0.58	0.838
	1b	12	150	12	30	5	30	5	5	5	12.5	0.58	0.593
	1c	12	12	150	30	30	5	5	5	5	1.0	0.58	0.864
Carbon/Epoxy $0^0/90^0$	2a	10	90	90	10	10	10	5	5	30	9.0	1.29	0.854
	2b	90	10	90	10	10	10	5	30	5	0.11	1.29	0.946
Carbon/Epoxy Quasi-isotropic	3a	10	60	60	10	30	30	5	5	20	6.0	0.19	0.512
	3b	60	10	60	30	10	30	5	20	5	0.17	0.19	0.695
C-SiC ceramic matrix composite	4a	20	120	120	23	9	9	8	8	20	6.0	2.49	0.971
	4b	120	20	120	9	23	9	8	20	8	0.17	2.49	0.982
Representative Isotropic Comp.	5	80	80	80	30	30	30	20	20	20	1.00	1.00	0.911
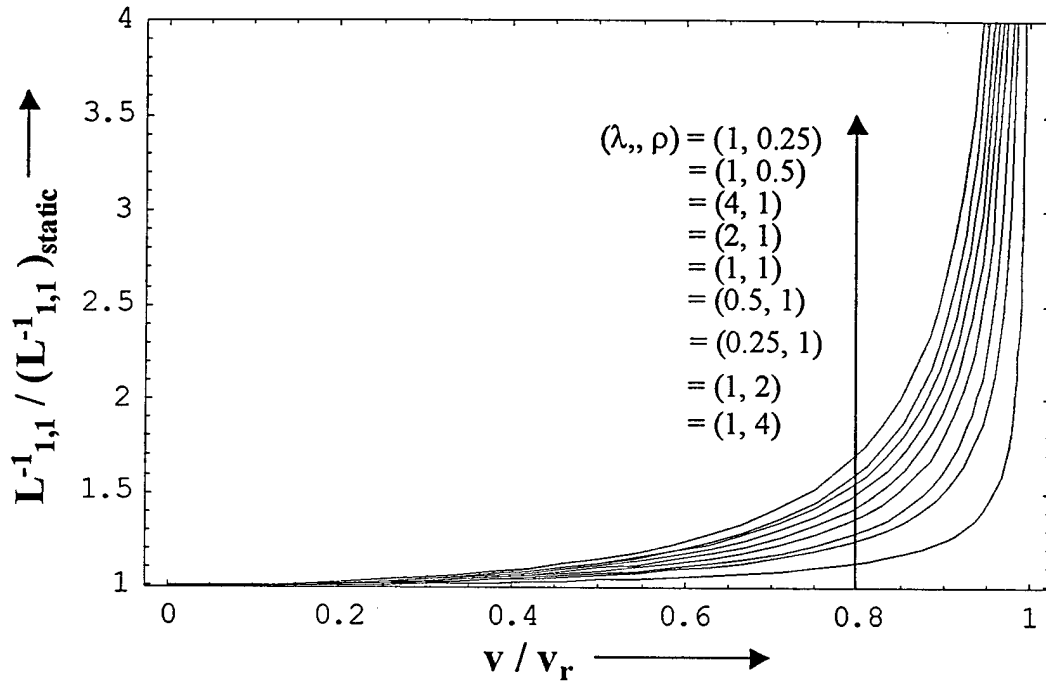
Figure 1: The variation of $L^{-1}_{1,1}$ normalized by the corresponding static value as a function of the crack tip velocity, normalized by the Rayleigh wave velocity, is shown for different values of λ and ρ.

Figure 2: The variation of $L^{-1}_{2,2}$ normalized by the corresponding static value as a function of the crack tip velocity, normalized by the Rayleigh wave velocity, is shown for different values of λ and ρ.
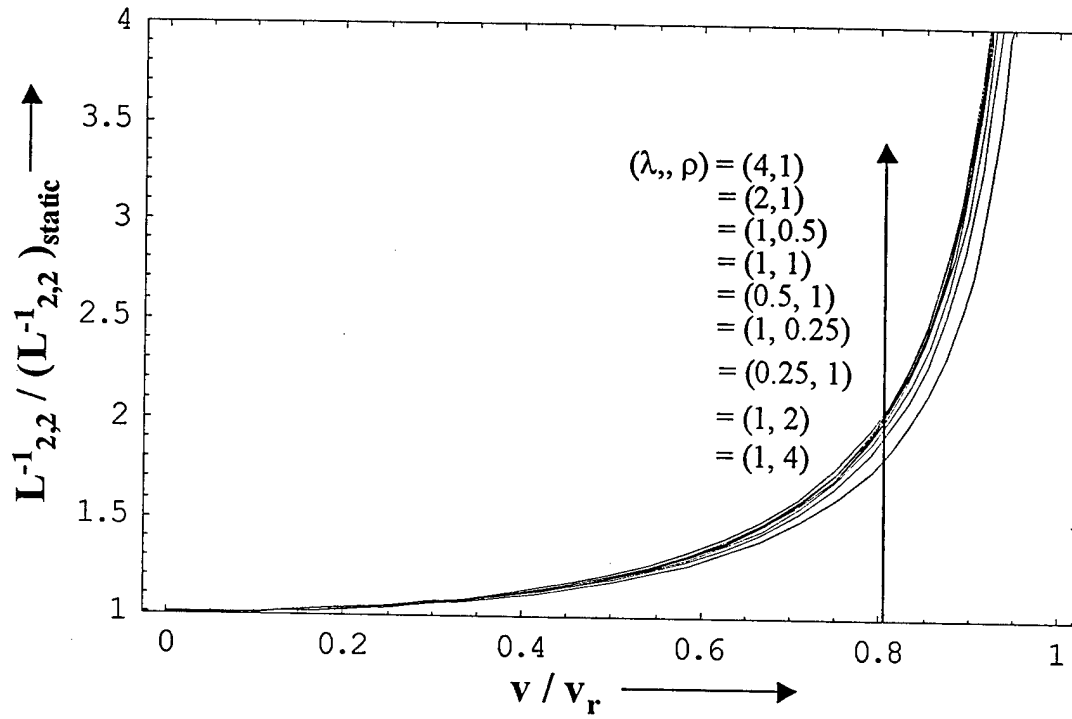
DYNAMIC DELAMINATION IN THROUGH THICKNESS REINFORCED DCB SPECIMENS

N. Sridhar[1*], I. J. Beyerlein[2], B. N. Cox[1] and R. Massabò[3]

[1]*Rockwell Science Center, 1049 Camino Dos Rios, Thousand Oaks, CA 91360, U.S.A.*
[2]*Los Alamos National Laboratory, New Mexico, U.S.A*
[3]*Department of Structural and Geotechnical Engineering, University of Genova, Italy*

ABSTRACT

Bridged crack models using beam theory formulation have proved to be effective in the modeling of quasistatic delamination crack growth in through thickness reinforced structures. In this paper, we model dynamic crack propagation in these structures with the beam theory formulation. Steady state crack propagation characteristics unique to the dynamic case are first identified. Dynamic crack propagation and the energetics of steady state dynamic crack growth for a Double Cantilever beam (DCB) configuration loaded with a flying wedge is next examined. We find that steady state crack growth is attainable for this loading configuration provided certain conditions are satisfied.

KEYWORDS
Dynamic, Delamination, Crack, Bridging, DCB, Stitching, Energy Release Rate

INTRODUCTION

Through thickness reinforcement of various kinds, including stitched or woven continuous fiber tows and metallic or fibrous short rods, has been developed to address the delamination problem in structural composite laminates. Substantial experimental evidence shows that through thickness reinforcement dramatically alters the delamination characteristics for the better under both static and dynamic loading conditions. For static loading, a fundamental theory based on observations of essential mechanisms is now mostly in place [1-6]. The mechanics of crack bridging by the through thickness tows has been mapped out, with governing length scales and material parameters identified [1-6]. However equivalent fundamental knowledge and models for dynamic delamination do not exist.

This paper deals with the delamination mechanics for through thickness reinforced structures under dynamic crack propagation conditions. A beam theory formulation is adopted and certain crack propagation characteristics are identified for mode I conditions. In the next section, we examine the energetics of crack growth for a through thickness reinforced DCB specimen loaded by a flying wedge. The double cantilever beam (DCB) specimen loaded dynamically by a flying wedge offers a relatively simple experimental approach to analyzing the mode I dynamic delamination problem. Regions of stable crack growth as a function of the material properties of the through thickness reinforcement, the size of the DCB specimen and the velocity of the wedge have been identified.

Beam Theory Formulation and Solution Characteristics:

For a beam element, the equations of motion are:

$$\frac{\partial N}{\partial x} = \rho B h \frac{\partial^2 u}{\partial t^2} \tag{1a}$$

$$\frac{\partial Q}{\partial x} - p(w,t)B = \rho B h \frac{\partial^2 w}{\partial t^2} \tag{1b}$$

$$\frac{\partial M}{\partial x} - Q = \rho I \frac{\partial^2 \phi}{\partial t^2} \tag{1c}$$

where $u(x,t)$ and $w(x,t)$ are the in-plane and transverse displacements of the neutral plane respectively, $\phi(x,t)$ is the clockwise rotation of the cross-section, t is the time variable, N is the axial force, Q is the shear force, M is the bending moment, $2h$ is the total thickness of the DCB specimen, B is the width of the specimen, ρ is the density, $I (= Bh^3/12)$ is the moment of inertia and $p(w,t)$ is the bridging traction corresponding to the opening mode. In this work, the time dependent bridging traction p corresponding to the opening mode is assumed to depend only on the transverse displacement w. In the absence of an axial force N, $u = 0$.

For a Timoshenko beam, the equations for steady state motion can be reduced to [7]:

$$\frac{\partial^4 w}{\partial X^4} + \frac{c_l^2}{(R-c_l^2)(1-c_l^2)} \frac{12R}{h^2} \frac{\partial^2 w}{\partial X^2}$$
$$- \frac{1}{(R-c_l^2)} \frac{1}{Eh} \frac{\partial^2 p(w,X)}{\partial X^2} + \frac{1}{(R-c_l^2)(1-c_l^2)} \frac{12R}{Eh^3} p(w,X) = 0 \tag{2a}$$

$$\frac{\partial \phi}{\partial X} = \frac{p(w,X)}{REh} - \frac{(R-c_l^2)}{R} \frac{\partial^2 w}{\partial X^2} \tag{2b}$$

where $X = x - vt$, $c_l^2 = \rho v^2 / E$, $R = \kappa G / E$, v is the (constant) steady state velocity, G and E are the shear modulus and the Young's modulus of the laminate and the dimensionless shear coefficient $\kappa=5/6$ for a beam with rectangular cross-section. For steady state dynamic delamination, the velocity v is the delamination crack tip velocity.

For an Euler-Bernoulli (E-B) beam, where both shear deformation and rotational inertia are ignored, the equation for steady state motion reduces to a simple form given by:

$$\frac{\partial^4 w}{\partial X^4} + \frac{12 c_l^2}{h^2} \frac{\partial^2 w}{\partial X^2} + \frac{12}{E h^3} p(w,X) = 0 \qquad (3)$$

Let us now consider a linear bridging law of the following type to represent the bridging action of the through thickness reinforcement:

$$p(w,X) = p_0 + \beta_3 w \qquad (4)$$

The linear law particularizes to the Dugdale law $p = p_0$ (for $\beta_3 = 0$) and to the proportional linear law $p = \beta_3 w$ (for $p_0 = 0$). In the results that follow, we non-dimensionalize the variables by the laminate thickness h ($w \equiv hW$, $u \equiv hU$ and $X \equiv h\xi$). Thus, the transverse displacement obeys:

$$\frac{\partial^4 W}{\partial \xi^4} + \beta^2 \frac{\partial^2 W}{\partial \xi^2} + b^2 W + d^2 = 0 \qquad (5)$$

For Timoshenko beam:

$$\beta = \sqrt{\frac{12 c_l^2 R}{(1 - c_l^2)(R - c_l^2)} - \frac{\beta_3 h}{(R - c_l^2)E}} \; ; \qquad b = \sqrt{\frac{R}{(1 - c_l^2)(R - c_l^2)} \frac{12 \beta_3 h}{E}} \; ;$$

$$d = \sqrt{\frac{R}{(1 - c_l^2)(R - c_l^2)} \frac{12 p_0}{E}} \; ; \qquad (6a)$$

For Euler-Bernoulli (E-B) beam:

$$\beta = \sqrt{12 c_l^2} \; ; \qquad b = \sqrt{\frac{12 \beta_3 h}{E}} \; ; \qquad d = \sqrt{\frac{12 p_0}{E}} \; ; \qquad (6b)$$

The general solution to Eqn. 5 is:

$$W(\xi) = -\frac{d^2}{b^2} + K_1 e^{-\sqrt{-\frac{\beta^2}{2} - \frac{1}{2}\sqrt{\beta^4 - 4b^2}} \, \xi} + K_2 e^{+\sqrt{-\frac{\beta^2}{2} - \frac{1}{2}\sqrt{\beta^4 - 4b^2}} \, \xi}$$

$$+ K_3 e^{-\sqrt{-\frac{\beta^2}{2} + \frac{1}{2}\sqrt{\beta^4 - 4b^2}} \, \xi} + K_4 e^{+\sqrt{-\frac{\beta^2}{2} + \frac{1}{2}\sqrt{\beta^4 - 4b^2}} \, \xi} \qquad (7)$$

There are three regimes to the solution behaviour which are independent of the boundary conditions, and these have been identified below (Note: $S = \beta_3 h / (12 \kappa G)$):

• Case 1: $\beta^2 < 0$ and $\beta^4 > 4b^2 \Rightarrow$ Exponential behavior
- For Timoshenko beam, this is true provided:

$$\frac{\rho v^2}{E} \le \frac{S}{1 + S} \quad \text{and} \quad 3(S(1 - c_l^2) - c_l^2)^2 \ge S(1 - c_l^2)(R - c_l^2) \qquad (8a)$$

- For the E-B beam, the above condition is never satisfied.
• Case 2: $\beta^2 > 0$ and $\beta^4 > 4b^2 \Rightarrow$ Oscillatory and non-decaying behavior
- For Timoshenko beam, this is true provided:

$$\rho v^2 / E > S / (1 + S) \quad \text{and} \quad 3(S(1 - c_l^2) - c_l^2)^2 \ge S(1 - c_l^2)(R - c_l^2) \qquad (8b.1)$$

- For the E-B beam, this condition is satisfied when: $\rho v^2 / E \ge 2\sqrt{S R}$ \qquad (8b.2)
• Case 3: $\beta^4 < 4b^2 \Rightarrow$ Oscillatory with exponential decay behavior
- For the Timoshenko beam, this is true when:

$$3\,(S(1-c_l^2)-c_l^2)^2 < S(1-c_l^2)(R-c_l^2) \tag{8c.1}$$

- For the E-B beam, this is true when: $\rho v^2 / E < 2\sqrt{S\,R}$ (8c.2)

The conditions determined above give us insight into when dynamic effects can significantly alter the mechanisms of deformation and the resultant bridging phenomena. For instance, if the crack tip velocity exceeds the condition prescribed in Eqn. 8a, oscillatory displacement fields will be introduced in the wake of the crack and these multiple oscillations could lead to crack face interpenetration. When such oscillations are present, the mechanics of bridging and the efficacy of through thickness bridging ligaments on the energetics of crack growth will be considerably altered. For example, stick-slip propagation modes would appear to be possible, as contacting fracture surfaces bounce. The complex details of such a possibility will be considered elsewhere. Here, we model the arms of the DCB specimen as a EB beam and study propagation characteristics up to the point of fracture surface contact, which is a simpler problem. (Constants β, b and d are given in Eqn.6b)

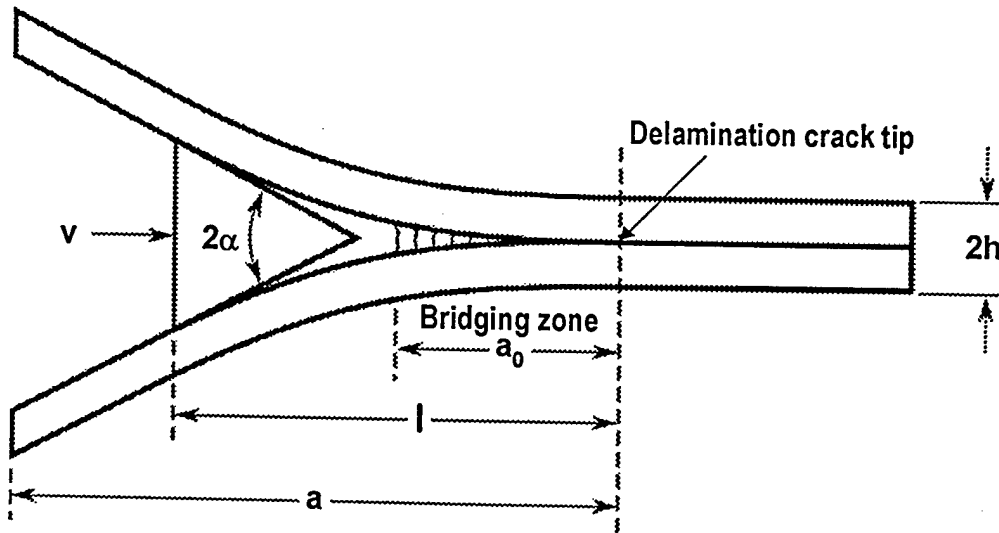## Wedge-Loaded Double Cantilever Beam

Figure 1: Schematic of through-thickness reinforced DCB specimen loaded with a flying wedge

The double cantilever beam (DCB) specimen loaded dynamically by a flying wedge, of constant velocity v, offers a relatively simple experimental approach to studying the mode I dynamic delamination problem (Fig. 1). The test is especially attractive for studying the bridging effects supplied by through-thickness reinforcement (e.g., stitches or rods) in laminates. In figure 1, 2α is the wedge angle, l is the distance between the wedge and the crack tip and a_0 is the length of the bridging zone. In non-dimensional form, $l \equiv h\,L$, and $a_0 \equiv h\,A_0$. The role of the bridging on the crack energy release rate is determined in this section. We assume that the crack propagates under steady state conditions and confirm the possibility of steady state propagation by finding consistent solutions. Further, we assume the bridging zone size is invariant and translates with the crack tip.

For the unbridged portion, the deflection profile ($w_u \equiv h\,W_u$) is obtained by setting $b = d = 0$. Therefore:

$$\frac{\partial^4 W_u}{\partial \xi^4} + \beta^2 \frac{\partial^2 W_u}{\partial \xi^2} = 0 \qquad \text{for } (-L \leq \xi \leq -A_0) \qquad (9a)$$

$$\frac{\partial^4 W}{\partial \xi^4} + \beta^2 \frac{\partial^2 W}{\partial \xi^2} + b^2 W + d^2 = 0 \qquad \text{for } (-A_0 < \xi \leq 0) \qquad (9b)$$

The relevant boundary conditions are:

$$W(\xi = 0) = 0, \ W'(\xi = 0) = 0, \ W_u'(\xi = -L) = -\alpha, \ W_u''(\xi = -L) = 0. \qquad (10)$$

The governing equation (9) together with the boundary conditions (10) and the continuity conditions at the end of the bridging zone ($\xi = -A_0$) will determine the deflection profile of the beam. Note that the bridging zone length (A_0) will be dictated by the critical crack opening displacement ($w_c \equiv h\,W_c$) required for failure of the bridging ligament. The crack energy release rate (G_{Total}), as determined through the total energy balance is:

$$G_{Total} = \frac{1}{B}\left(\frac{\partial U_{ext}}{\partial a} - \frac{\partial U_s}{\partial a} - \frac{\partial U_k}{\partial a} \right) \qquad (11)$$

where U_{ext} is the work done by the applied load, U_s is the strain energy, U_k is the kinetic energy, B is the uniform width of the DCB specimen, and a is the crack length. For steady state crack extension $a = vt$, where v is the crack velocity and t is time. For the DCB specimen loaded with a flying wedge this reduces to:

$$G_{Total} = \frac{\alpha E h}{6}\frac{\partial^3 W_u}{\partial \xi^3}\bigg|_{\xi = -L} - \rho h v^2 \alpha^2 \qquad (12)$$

In addition, by application of the dynamic J-integral, the energy released at the crack tip is related to the bending moment M by [8]:

$$G_{Tip} = \frac{12}{E h^3}\left[M_{\xi=0} \right]^2 = \frac{Eh}{12}\left(\frac{\partial^2 W}{\partial \xi^2}\bigg|_{\xi=0} \right)^2 \qquad (13)$$

In general, due to crack bridging, $\Delta G = G_{Total} - G_{Tip} \neq 0$. The energy difference, ΔG, is the extra work done in fracturing the bridging ligaments. For the linear bridging law, we find that the shielding contribution ΔG from the bridging ligaments is:

$$\Delta G = G_{Total} - G_{Tip} = 2 \int_{-W_c}^{0} p\, du \qquad (14)$$

This result is identical to what we obtain in the quasi-static case for small scale bridging conditions. Since there is no rate dependence to the bridging law, it is not surprising that the small scale bridging limit relationship is obeyed.

Since we limit our analysis to small scale bridging, tow failure must occur in the wake of the crack. Small scale bridging is ensured provided the displacement profile monotonically increases within the bridging zone from the crack tip and the pull-out required for tow failure is less than the maximum crack opening displacement within the bridging zone. This condition determines a criterion for the

maximum allowable bridging zone length, A_{max} , which is obtained by solving $\partial W(\xi = -A_{max})/\partial\xi = 0$. Therefore, if $A_0 \leq A_{max}$, then $W_c \leq W_{critical}(\equiv W(\xi = -A_{max}))$, and hence small scale bridging condition is ensured.

Detailed calculations of the deflection profile, the crack energy release rate and the maximum allowable bridging length can be computed with the formalism presented above for both the Dugdale bridging law and the proportional bridging law. For instance, when the bridging ligaments obey the Dugdale bridging law, steady state crack propagation with small scale bridging is provided $A_0 \leq A_{max}$, where A_{max} is given by:

$$-2\lambda\left(Cos(\lambda) - Cos(\lambda(1-\hat{A}_{max}))\right) + 2\lambda D\,\hat{A}_{max}\left(Cos(\lambda(1-\hat{A}_{max})) - 1\right)$$
$$+D\left(Sin(\lambda(1-2\hat{A}_{max})) + Sin(\lambda\,\hat{A}_{max})\right) + D\left(Sin(\lambda\,\hat{A}_{max}) - Sin(\lambda)\right) = 0 \quad (15)$$

and where $\lambda = \beta L$, $D \equiv d/\lambda$, and $\hat{A}_{max} \equiv A_{max}/L$. Regions of steady state stable crack growth under small scale bridging condition can thus be deduced as a function of the material properties of the through thickness reinforcement, the size of the DCB specimen and the velocity of the wedge.

CONCLUSIONS

The dynamic delamination cracking behavior and the energetics of crack growth in through thickness double cantilever beam (DCB) specimens has been analyzed. The role of bridging by stitches or rods in dynamic crack growth was computed by solving the bridged crack problem within the framework of beam theory. For steady state crack growth conditions, different regimes of the solution behavior have been identified which would correspond to different crack propagation characteristics. Regions of steady state crack growth under small scale bridging condition can be deduced as a function of the material properties of the through thickness reinforcement, the size of the DCB specimen and the velocity of the wedge. This provides guidelines for design of experiments to probe the efficacy of bridging on improving the dynamic fracture toughness of through thickness reinforced structures.

REFERENCES:

1. Cartié, D. D. R., and Partridge, I. K., "Z-Pinned Composite Laminates: Improvements in Delamination Resistance," *Proc. DFC5 Conference*, I. Mech. E., March, 1999.
2. Jain, L.K., Mai, Y-W. (1994), Analysis of stitched laminated ENF specimens for interlaminar mode-II fracture toughness, *Int. Journal of Fracture* **68**(3), 219-244.
3. M. He and B. N. Cox, "Crack Bridging by Through-Thickness Reinforcement in Delaminating Curved Structures," *Composites A*, 29[4] 377-93 (1998).
4. R. Massabò and B. N. Cox, "Concepts for Bridged Mode II Delamination Cracks," *J. Mech. Phys. Solids*, **47**, 1265-1300 (1999).

5. B. N. Cox, "Constitutive Model for a Fiber Tow Bridging a Delamination Crack," *Mechanics of Composite Materials and Structures,* in press.

6. R. Massabò and B. N. Cox, "Unusual Characteristics of mixed mode delamination fracture in the presence of large scale bridging," *Mech. Comp. Mater. Structures,* in press

7. N.Sridhar, I.J.Beyerlein, B.N.Cox and R. Massabò, "Delamination mechanics in Through-Thickness Reinforced Structures under dynamic crack growth conditions," *in prepn.*

8. L.B.Freund, "Dynamic Fracture Mechanics," *Cambridge University Press,* New York (1993)

ICF100414OR

BEAM THEORY AND WEIGHT FUNCTION METHODS FOR MODE I DELAMINATION WITH LARGE SCALE BRIDGING

R. Massabò[1] and B. N. Cox[2]

[1] Department of Structural and Geotechnical Engineering, University of Genova,
Genova, 16145, Italy
[2] Rockwell Science Center, Thousand Oaks, CA 91360, USA

ABSTRACT

A nonlinear fracture mechanics model is formulated for analysis of mode I delamination of orthotropic double cantilever beam specimens in the presence of large scale bridging conditions. The problem is solved using a nonlinear integral equation approach in terms of stress intensity factors at the crack tip. An approximate weight function is proposed and validated numerically for a pair of concentrated forces acting on the surfaces of the delamination. The model accounts for the presence of regions of contact along the wake of the crack, which may form due to the action of the bridging mechanisms. The influence of the orthotropy of the material on the fracture behavior is investigated and the validity of approximated solutions based on beam theory is checked.

KEYWORDS: Nonlinear fracture mechanics, delamination, strengthening mechanisms, anisotropic material, large scale bridging.

INTRODUCTION

Mode I and mixed mode delamination in large scale bridging conditions, such as those created by through thickness reinforcement in composite laminates, shows unusual phenomena of crack face closure, crack arrest and crack propagation with crack face contact, which have no precedent in the delamination of conventional tape laminates [1,2]. In [3] the authors considered a typical mixed mode geometry, the Mixed Mode Bending specimen proposed by Crews and Reeder, and explained these phenomena by means of a simple analytical model based on Timoshenko beam theory. The model treats the delaminated arms of the specimen as beams on an elastic, generally nonlinear, foundation of Winkler type with the constitutive laws of the springs given by the bridging law, which characterizes the bridging mechanism. The crack

closure phenomenon is a manifestation of the oscillations of the function representing the deflection of the beams in the wake of the crack. The wavelength of the function, λ, sets the characteristic length scale of the problem, which in the case of linear bridging mechanisms is given approximately by $\lambda/4 = \pi/2 \sqrt[4]{4k_d / \beta_3}$, with β_3 the modulus of the foundation and k_d the flexural stiffness of the beam cross section. Once the limit configuration for crack tip closure is approached, the fracture response of the specimen will depend on the geometry and the loading conditions. In the case of a specimen symmetric about its midplane and in the absence of mode II loading, the crack will stop and the specimen will break by mechanisms other then delamination. In the presence of mode II loading or in asymmetric specimens, the crack will continue to propagate and the propagation will be opposed not only by the bridging mechanism but also by friction acting in the regions of contact.

The model proposed in [3] explains qualitatively all the problems associated with large scale bridging delamination. However, the model makes strong assumptions which could affect the solutions quantitatively, namely it schematizes the specimen as a one-dimensional structure, it neglects the influence of the elastic material in front of the crack (built-in ends assumption) and it deals only approximately with regions of contact between the delaminated faces and the effect these regions may have on crack propagation driven by mode II loading.

In this paper a nonlinear fracture mechanics model is formulated for analysis of delamination crack growth which removes the above mentioned assumptions, assumes a two-dimensional deformation field and accounts for the orthotropy of the material. The problem is solved through an integral equation approach in terms of stress intensity factors at the crack tip. Since the crack closure phenomenon is controlled by the mode I response of the laminate, focus in this initial work is restricted to the problem of a double cantilever beam.

FRACTURE PARAMETERS IN ORTHOTROPIC DOUBLE CANTILEVER BEAMS

Stress intensity factors

An exact solution for the stress intensity factor K_{IP} due to a pair of concentrated forces P applied per unit width onto the crack faces of a double cantilever beam at a distance d from the crack tip has been obtained by Foote and Buchwald [4]. They solved the problem by applying the Wiener-Hopf technique to an isotropic, arbitrarily loaded infinite strip and representing the concentrated loads in terms of the Dirac delta function. A simple formula approximating the exact solution, which has an accuracy of 1.1% and can be applied to double cantilever beams with an uncracked ligament $c > 2h$, is also given in [4]:

$$\frac{K_{IP}h^{0.5}}{P} = \sqrt{12}\left(\frac{d}{h}+0.673\right)+\sqrt{\frac{2h}{\pi d}}-\left[0.815\left(\frac{d}{h}\right)^{0.619}+0.429\right]^{-1} \tag{1}$$

where h is the half thickness of the specimen. For large d/h, Eq. (1) approaches the elementary beam theory solution of a double cantilever beam with built-in ends, $K_I h^{0.5}/P = \sqrt{12}\, d/h$ [3]. For $d/h \geq 0.3$ the exact K_{IP} is well represented (error always lower than 4%) by Gross and Srawley's boundary collocation solution, approximately given by the first bracket term on the right hand

side. The same limit solution is given by the modified beam theory of Kanninen, which removes the assumption of built-in ends to account for the elasticity of the uncracked ligament. For very small d/h the dimensionless K_{IP} of Eq. (1) approaches Irwin's solution for a semi-infinite crack in an infinite sheet, $K_I h^{0.5}/P = (2/\pi\, h/d)^{0.5}$. A lower limit for the normalized crack length a/h of the double cantilever beam specimen must be set for Eq. (1) to be valid for all d/h, $0 < d/h \le a/h$. Irwin's solution for very small d/h is correct only if $a \gg d$, and should be replaced by Tada's solution [5] for a finite crack of length a in a semi-infinite sheet when a/h also becomes very small. A conservative lower limit for a/h can be set as $a/h \ge 0.3$, so that when $d/h = a/h = 0.3$, Gross and Srawley's solution is already approached.

The stress intensity factor due to a pair of concentrated forces P_i applied on the crack faces of an orthotropic double cantilever beam at the coordinate $x_1 = x_{1i}$ (Fig. 1.a) can be deduced from the expression of the strain energy release rate G_I obtained by Suo et al. [6] making use of the orthotropic relationship $K_{Ii} = \sqrt{G_I E_1'}$. Plane stress conditions are assumed along with a principally orthotropic material with $E_1' = (\sqrt{2E_1 E_3}\,\lambda^{1/4})/\sqrt{1+\rho}$, $\lambda = E_3/E_1$ and $\rho = \sqrt{E_1 E_3}/2G_{13} - \sqrt{\nu_{13}\nu_{31}}$ the orthotropic ratios [6], E_1 and E_3 the Young's moduli in the x_1 and x_3 directions, G_{13} the shear modulus and ν_{13} and ν_{31} Poisson's ratios. The dimensionless stress intensity factor is then given by:

$$\frac{K_{Ii} h^{0.5}}{P_i} = \frac{\lambda^{3/8}}{\sqrt{n}}\sqrt{12}\left(\frac{a - x_{1i}}{h} + Y_I(\rho)\lambda^{-1/4}\right) \tag{2}$$

where:

$$Y_I(\rho) = 0.677 + 0.146(\rho - 1) - 0.0178(\rho - 1)^2 + 0.00242(\rho - 1)^3 \tag{3}$$

and $n = \sqrt{(1+\rho)/2}$. For an isotropic material ($\lambda = \rho = 1$), $Y_I(\rho) = 0.677$ and Eq. (2) coincides with Gross and Srawley's solution. The last term on the right hand side of eq. (2) describes the influence of the elasticity of the uncracked ligament ahead of the crack tip and it vanishes for large $(a-x_{1i})/h$, when the solution for an orthotropic beam with built-in ends is recovered. Equation (2), as well as the expression of G_I from which it was derived, has 1% accuracy for all $(a-x_{1i})/h \ge 2\lambda^{-1/4}$ and $0 \le \rho \le 4$.

An exact solution for the stress intensity factor K_{Ii} when $(a-x_{1i})/h < 2\lambda^{-1/4}$ is not available in the literature. However, examination of Eqs. (1) and (2) along with the observation that Irwin's solution for very small $d/h = (a-x_{1i})/h$ maintains its validity also in orthotropic sheets [7], suggests the following formula:

$$\frac{K_{Ii} h^{0.5}}{P_i} = \frac{\lambda^{3/8}}{\sqrt{n}}\sqrt{12}\left(\frac{a - x_{1i}}{h} + Y_I(\rho)\lambda^{-1/4}\right) +$$

$$\sqrt{\frac{2h}{\pi(a - x_{1i})}} - \left[0.815\left(\frac{a - x_{1i}}{h}\right)^{0.619} + \frac{\sqrt{n}}{\lambda^{1/8}\sqrt{12}Y_I(\rho)}\right]^{-1} \tag{4}$$

which has the right asymptotic behaviors for large and small $(a-x_{1i})/h$. The validity of Eq. (4) for intermediate values of $(a-x_{1i})/h$ has been checked through finite element calculations for a range of λ and ρ typical of composite laminates, $0.025 \leq \lambda \leq 1$ and $0 \leq \rho \leq 4$, and the relative error has been found to be always lower than 4%. The lower limit for the normalized crack length for which Eq. (4) is valid can be defined by referring to the limit for an isotropic material and exploiting orthotropic rescaling of lengths [6], which yields $a/h \geq 0.3\ \lambda^{-1/4}$. When a reason exists for studying very small cracks as well as non-small cracks in numerical work, Eq. (4) can be combined very easily with Tada's result for the appropriate domains of a/h.
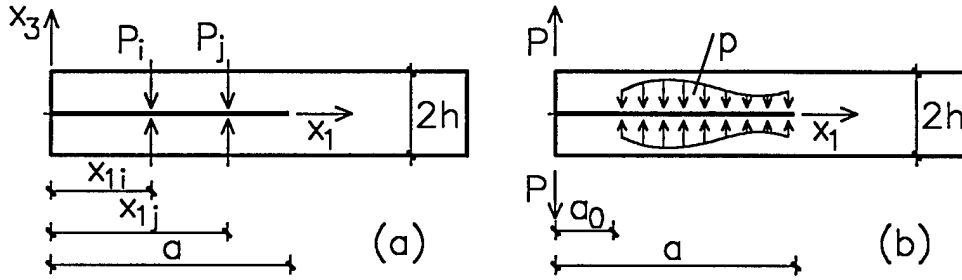

Figure 1: Schematic of the DCB specimen under different loading conditions.

Crack opening displacement

The crack opening displacement u_3 at the coordinate x_{1i} due to a pair of opening forces P_j acting at x_{1j}, Fig. 1, is obtained from the localized compliance $\lambda_{ij} = u_3(x_{1i})\ /\ P_j$ which can be defined through an energy balance or Castigliano's theorem as shown in [8] for an isotropic body. The localized compliance is given by:

$$\lambda_{ij} = \frac{u_3(x_{1i})}{P_j} = \frac{2}{E_1'} \int_0^a \frac{K_{Ii}(a,x_{1i})K_{Ij}(a,x_{1j})}{P_i P_j}\,da \qquad (5)$$

where E_1' is the orthotropic constant defined above, P_i is a pair of fictitious forces acting at x_{1i}, and K_{Ii} and K_{Ij} are the stress intensity factors at the crack tip due to P_i and P_j, respectively, given by Eq. (4).

ORTHOTROPIC DOUBLE CANTILEVER BEAM WITH LARGE SCALE BRIDGING

The stress intensity factor at the crack tip of a double cantilever beam with tractions p acting along the bridged portion of the crack as shown in Fig. 1.b is given by:

$$K_I = K_{IP} + K_{Ip} = K_{IP} - \int_{a_0}^a \frac{K_{Ii}(a,x_{1i})}{P_i}\,p[u_3(x_{1i})]dx_i \qquad (6)$$

where a_0 is the unbridged length of the crack, K_{IP} is the stress intensity factor due to the external loads P acting at $x_{1i} = 0$, and K_{Ip} is the stress intensity factor due to opening tractions p; K_{Ii}/P_i

represents the Green's function of the problem and is given by Eq. (4). The tractions p depend on the crack opening displacement and are a priori unknown in Eq. (6). If $u_3(x_{1i}) > 0$, then $p[u_3(x_{1i})] = p_3[u_3(x_{1i})]$ is the closing traction developed by the bridging mechanisms. The value of p_3 as a function of u_3 is defined through the bridging traction law, $p_3(u_3)$, which is one of the data of the model. If $u_3(x_{1i}) = 0$, then $p[u_3(x_{1i})] = -p_c[(x_{1i})]$ is the opening traction depicting the effect of the contact pressure. The contact pressure and the size of the regions of contact are unknown a priori and can be determined through a compatibility condition for the crack opening displacement.

The crack opening displacement $u_3(x_{1i})$ is obtained by applying the superposition principle and Eq. (6):

$$u_3(x_{1i}) = u_3(x_{1i})_P + u_3(x_{1i})_p = \lambda_{iP}P - \int_{a_0}^{a} \lambda_{ij} p[u_3(x_{1j})]\,dx_j \qquad (7)$$

which yields:

$$\frac{u_3(x_{1i})}{h} = \frac{2P}{E_1'h} \int_0^{a/h} \frac{K_{IP}(a/h)h^{0.5}}{P} \frac{K_{Ii}(a/h, x_{1i}/h)h^{0.5}}{P_i} d(\frac{a}{h})$$

$$- \frac{2}{E_1'} \int_{a_0/h}^{a/h} \int_{\max[x_{1i}/h, x_{1j}/h]}^{a/h} \frac{K_{Ii}(a/h, x_{1i}/h)h^{0.5}}{P_i} \frac{K_{Ij}(a/h, x_{1j}/h)h^{0.5}}{P_j} d(\frac{a}{h}) p[u_3(x_{1j}/h)]d(\frac{x_{1j}}{h})$$

$$(8)$$

Note that the dimensionless K_I's appearing in Eq. (8) and in the equations that follow depend also on the orthotropic ratios, λ and ρ, as shown in Eq. (4).

Crack propagation in large scale bridging

At the onset of crack propagation the crack tip stress intensity factor of Eq. (6) is equal to the intrinsic fracture toughness, $K_I = K_{Ic}$, and the dimensionless critical load for crack propagation takes the form:

$$\frac{P_{cr}}{K_{Ic}h^{0.5}} = \cfrac{1}{\cfrac{K_{IP}(a/h)h^{0.5}}{P}\left\{1 + \frac{p_{30}h^{0.5}}{K_{Ic}} \int_{a_0/h}^{a/h} \left[\frac{K_{Ii}(a/h, x_{1i}/h)h^{0.5}}{P_i}\right] \frac{p[u(x_{1i}/h)]}{p_{30}} d(\frac{x_{1i}}{h})\right\}} \qquad (9)$$

where p_{30} is a normalizing value of the crack face tractions, p_3, given for instance by their maximum value. The dimensionless number on the right hand side of Eq. (9), $p_{30}h^{0.5}/K_{Ic}$, is a measure of the brittleness of the structure. Recalling the expression for E_1' and that $K_{Ic} = \sqrt{G_{Ic}E_1'}$, Eq. (9) can be modified to allow direct comparison between isotropic and othotropic cases:

$$\frac{P_{cr}}{\sqrt{G_{Ic}E_1 h}} = \frac{\lambda^{3/8}}{\sqrt{n}} \frac{1}{\dfrac{K_{IP}(a/h)h^{0.5}}{P}}$$
$$\left\{ 1 + \frac{p_{30}h^{0.5}}{\sqrt{G_{Ic}E_1}} \int_{a_0/h}^{a/h} \left[\frac{K_{Ii}(a/h, x_{1i}/h)h^{0.5}}{P_i} \right] \frac{p[u(x_{1i}/h)]}{p_{30}} d(\frac{x_{1i}}{h}) \right\} \tag{10}$$

The normalized crack opening displacement at the generic coordinate x_{1i} is obtained substituting $P = P_{cr}$ into Eq. (8):

$$\frac{u_3(x_{1i})E_1'}{K_{Ic}h^{0.5}} = 2 \frac{P_{cr}}{K_{Ic}h^{0.5}} \int_0^{a/h} \frac{K_{IP}(a/h)h^{0.5}}{P} \frac{K_{Ii}(a/h, x_{1i}/h)h^{0.5}}{P_i} d(\frac{a}{h}) - 2 \frac{p_{30}h^{0.5}}{K_{Ic}}$$
$$\int_{a_0/h}^{a/h} \int_{\max[x_{1i}/h, x_{1j}/h]}^{a/h} \frac{K_{Ii}(a/h, x_{1i}/h)h^{0.5}}{P_i} \frac{K_{Ij}(a/h, x_{1j}/h)h^{0.5}}{P_j} d(\frac{a}{h}) \frac{p[u(x_{1j}/h)]}{p_{30}} d(\frac{x_{1j}}{h}) \tag{11}$$

The statically indeterminate problem defined by the nonlinear integral equations (8) and (9) is solved for general bridging laws, $p_3(u_3)$, through a discretization. A self-consistent solution for the crack profile is obtained iteratively through a numerical procedure following the approach of [8,9].

Dugdale type bridging law, $p_3 = p_{30}$

In the special case of bridging mechanisms described by a Dugdale type bridging law, $p_3 = p_{30}$, Eqs. (9) and (8) simplify and Eq. (9) alone gives the dimensionless critical load for crack propagation. Beam theory predicts the absence of regions of contact for this case and this qualitative characteristic is confirmed by the more accurate calculations of the integral equation approach. Setting aside for this paper the interesting question of the nature of contact regions when they do occur (e.g., for linear bridging laws), a detailed assessment is made here of the limitations of elementary beam theory for predicting crack propagation in the presence of large scale bridging.

Figures 2.a, 2.b and 2.c show dimensionless diagrams of the critical load for crack propagation as a function of the normalized crack length in a double cantilever beam specimen with $a_0 = 0$. As already noted the curves are correct only for $a/h \geq 0.3\ \lambda^{-1/4}$. Three different values of p_3 are considered, as marked. The curves named (a), (b) and (c) in each diagram describe the response of an isotropic material, an orthotropic material with $\lambda = 0.1$ and $\rho = 3$ (e.g. a graphite epoxy laminate) and an orthotropic material with $\lambda = 0.05$ and $\rho = 5$ (e.g. a boron-epoxy laminate), respectively. The dashed curves depict the elementary beam theory solution (built-in ends, negligible shear deformations). The dotted curve in Fig. 2b, obtained using Timoshenko beam theory for an isotropic material, highlights the influence of the shear deformations.
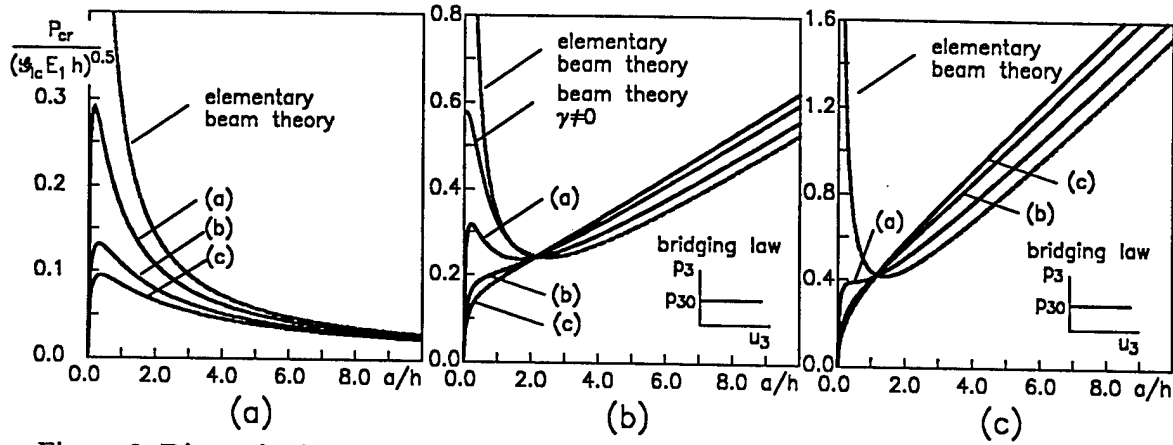
Figure 2: Dimensionless critical load versus normalized crack length in orthotropic DCB specimens. (a) No bridging. (b) Bridging tractions $p_3 = 0.1\sqrt{G_{Ic}E_1/h}$. (c) Bridging tractions $p_3 = 0.3\sqrt{G_{Ic}E_1/h}$.

Figure 2.a confirms the validity of elementary beam theory in unreinforced specimens when a/h is sufficiently high. The anisotropy of the material affects the response only for relatively small values of a/h. The influence of the anisotropy of the material on the structural response apparently seems to be more marked in members reinforced through the thickness (Figs. 2.b and 2.c). In this case, two different regimes of behavior are delineated by a transition value of $a/h = 1/(1.73 p_{30}\sqrt{G_{Ic}E_1/h})^{0.5}$, corresponding to the point where all curves cross each other. If a/h is smaller than the transition value, the anisotropy of the material strongly affects the response and the elementary beam theory solution does not describe the actual behavior even qualitatively. For a/h larger than the transition value, all curves tend to become parallel with a common slope given by $1/2\ p_{30}\sqrt{G_{Ic}E_1/h}$ and the deviation between the correct solution and the elementary beam theory solution becomes independent of the crack length and given by $1/2Y_I(\rho)\lambda^{-1/4} p_{30}\sqrt{G_{Ic}E_1/h}$. However, the fractional error is $Y_I(\rho)\lambda^{-1/4}/(a/h)$, which is independent of the intrinsic fracture toughness of the laminate, G_{Ic}, and the magnitude of the bridging tractions and coincides with the analogous fractional error of the case with no bridging. It depends only the crack length and the degree of anisotropy. This error is due to the assumption of neglecting the influence of the elastic material ahead of the crack tip and could be removed by using a modified beam theory (Kanninen's, Williams's).

CONCLUSIONS

An approximate weight function has been proposed and validated numerically for a pair of point forces acting on the surfaces of a delamination crack in a possibly thin orthotropic body. The weight function allows mode I large scale bridging problems in beams and plates to be formulated as integral equations without the limitations imposed on accuracy by beam theory approximations. In particular, the crack tip singularity will be properly represented. The integral equations can be solved using well-known, computationally efficient and accurate methods. The

weight function strongly depends on the anisotropy ratio. This is a feature of the plate or beam geometry.

The first application of the new weight function to the problem of a large zone of uniform bridging tractions (the Dugdale bridging model) shows the ranges of crack lengths over which beam theories of different order succeed and fail. The presence of large scale bridging is found not to significantly increase the sensitivity of the solutions to the degree of anisotropy with respect to the case with no bridging.

While elementary beam theory will always be correct for sufficiently large crack lengths, a/h, there is a regime of small crack lengths, $a/h \lesssim 2$, where rigorous solutions are required, e.g. based on integral equation methods. Moreover, there is a regime of practical interest for laboratory specimens, $2 \lesssim a/h \lesssim 10$, where elementary beam theory yields only qualitatively correct trends and solutions based on integral equation methods or on modified beam theory are required for quantitative accuracy.

REFERENCES

1. D.D.R. Cartié and I.K. Partridge, (1999), Delamination Behaviour of z-Pinned Laminates, *Proc. ICCM12*, Paris, July, 1999, ed., T. Massard, Woodhead Publishing Limited, Melbourne.
2. Rugg, K.L., Cox, B.N. and Massabò, R. (2000), Mixed mode delamination of polymer composite laminates reinforced through the thickness by z-fibers, submitted to *Composites, part A*.
3. Massabò R. and B.N. Cox (2000), Unusual characteristics of mixed mode delamination fracture in the presence of large scale bridging, *Mech. Comp. Mater. Structures*, in press.
4. Foote, R. M. L., and Buchwald, V.T., (1985), An exact solution for the stress intensity factor for a double cantilever beam, *Int. J. of Fracture*, 29, 125-134.
5. Tada, H. (1985) *The Stress Analysis of Cracks Handbook*. Paris Productions Inc., St. Louis, Missouri.
6. Suo, Z., Bao, G., Fan, B., and Wang, T.C., (1991), Orthotropy rescaling and implications for fracture in composites, *Int. J. Solids Structures*, 28(2), 235-248.
7. Sih, G.C., Paris, P.C., and Irwin, G.R., (1965), On cracks in rectilinear anisotropic bodies, *Int. J. of Fracture*, 1, 189-203.
8. Massabò, R., (1999), The bridged-crack model, book chapter in *Nonlinear Crack Models for Nonmetallic Materials*, (ed. A. Carpinteri), Solid Mechanics and its Applications Series (ed. G. Gladwell), Kluwer Academic Publishers, Dordrecht, The Netherlands, pp. 141-208.
9. Cox, B.N., and Marshall, D.B. (1991a) Stable and unstable solutions for bridged cracks in various specimens. *Acta Metall. Mater.* **39**, 579-89.